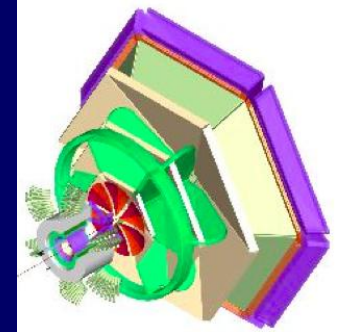


Deeply Virtual Exclusive Reactions with CLAS



Valery Kubarovsky
Jefferson Lab

Trento, Italy
October 14 , 2010

**Jefferson Lab**
Thomas Jefferson National Accelerator Facility

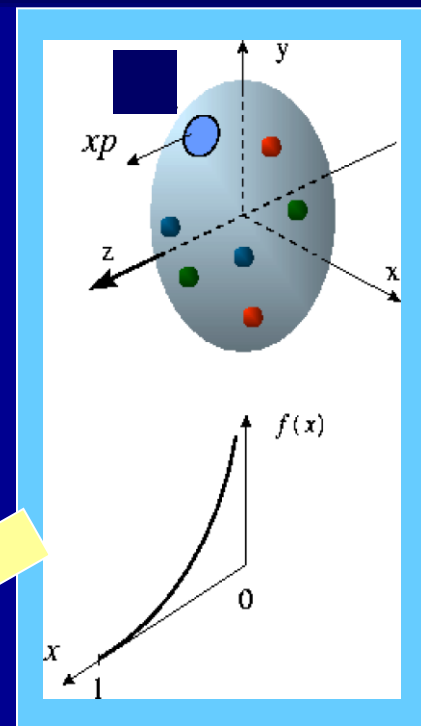
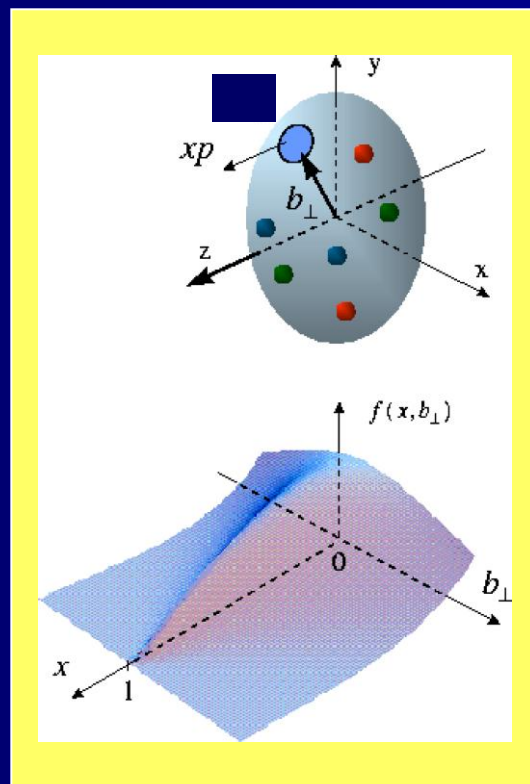
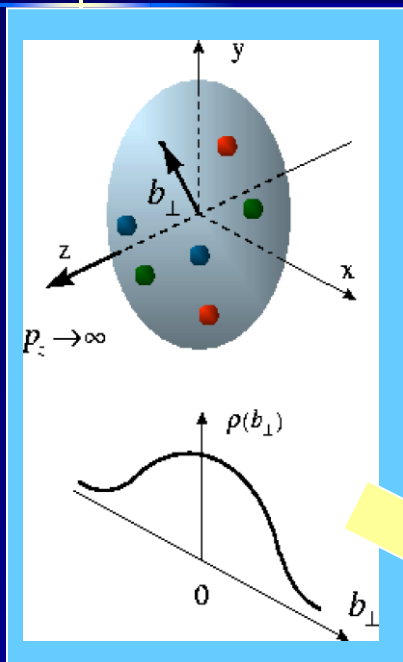
Outline

- Introduction
- DVMP theoretical models
- Brief update on DVCS
- π^0/η electroproduction
 - Cross sections
 - Structure functions
 - Beam spin asymmetry
 - Cross sections ratio
- Summary

How are the proton's charge densities related to its quark momentum distribution?

D. Mueller, X. Ji, A. Radyushkin, ... 1994 -1997

M. Burkardt, A. Belitsky... Interpretation in impact parameter space

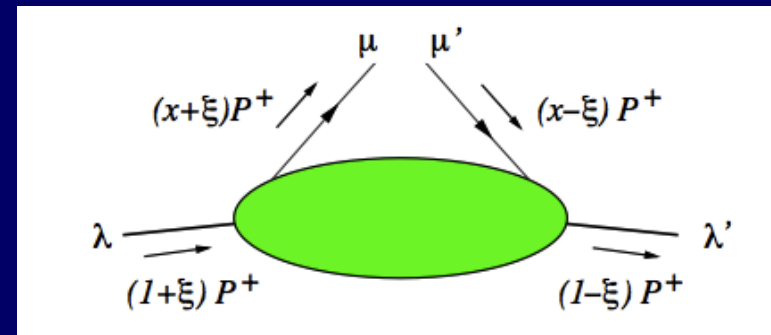


Proton form factors,
transverse charge &
current densities

Correlated quark momentum
and helicity distributions in
transverse space - **GPDs**

Structure functions,
quark **longitudinal**
momentum & spin
distributions

Generalized Parton Distributions



- There are 4 GPDs where partons do not transfer helicity $H, \tilde{H}, E, \tilde{E}$
- H and E are “unpolarized” and \tilde{H} and \tilde{E} are “polarized” GPD. This refers to the parton spins.
- 4 GPDs flip the parton helicity $H_T, \tilde{H}_T, E_T, \tilde{E}_T$

Basic GPD properties

- Forward limit

$$\begin{aligned}H^q(x, 0, 0) &= q(x) \\ \tilde{H}^q(x, 0, 0) &= \Delta q(x) \\ H_T^q(x, 0, 0) &= h_1^q(x)\end{aligned}$$

- Form factors

$$\begin{aligned}\int_{-1}^1 dx H^q(x, \xi, t) &= F_1^q(t), & \int_{-1}^1 dx E^q(x, \xi, t) &= F_2^q(t) \\ \int_{-1}^1 dx \tilde{H}^q(x, \xi, t) &= g_A^q(t), & \int_{-1}^1 dx \tilde{E}^q(x, \xi, t) &= g_P^q(t),\end{aligned}$$

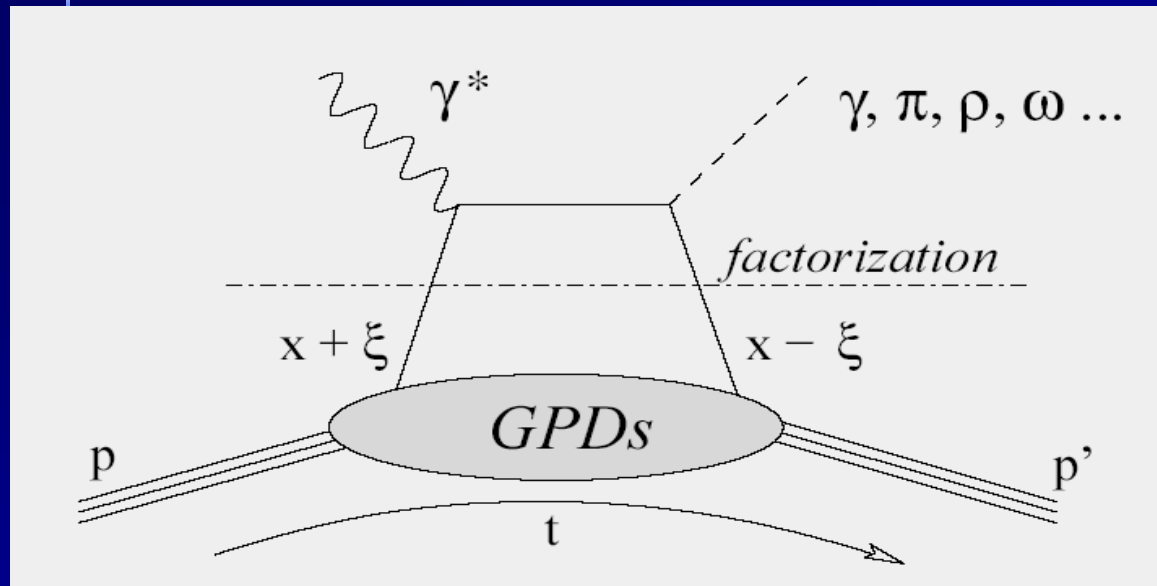
- Angular Momentum

$$J^q(t) = \frac{1}{2} \int_{-1}^1 dx x [H^q(x, \xi, t) + E^q(x, \xi, t)]$$

(Ji's sum rule)

Basic Process – Handbag Mechanism

Deeply Virtual Compton Scattering (DVCS)
Deeply Virtual Meson Production (DVMP)



x - longitudinal quark momentum fraction

2ξ - longitudinal momentum transfer

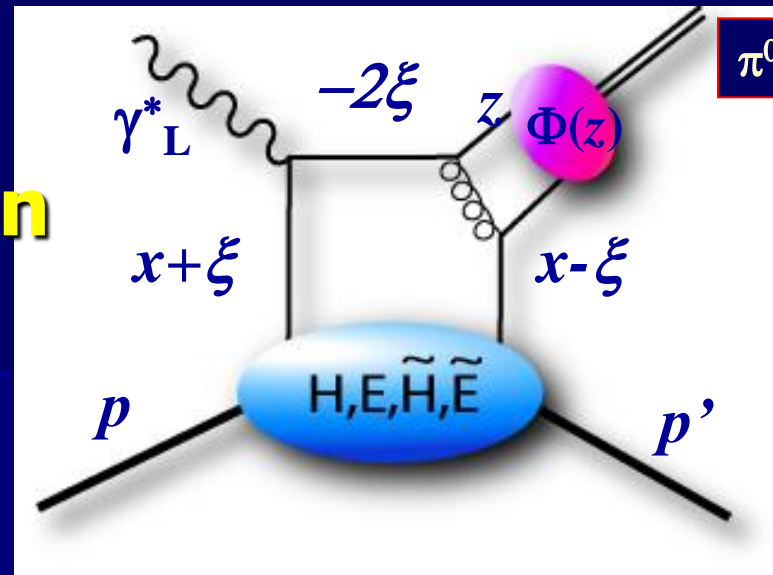
$\sqrt{-t}$ - Fourier conjugate to transverse impact parameter

➔ GPDs depend on 3 variables, e.g. $H(x, \xi, t)$. They probe the quark structure at the amplitude level.

$$\xi = \frac{x_B}{2-x_B}$$

High Q^2 , Low t Region

Collins, Frankfurt, Strikman - 1997



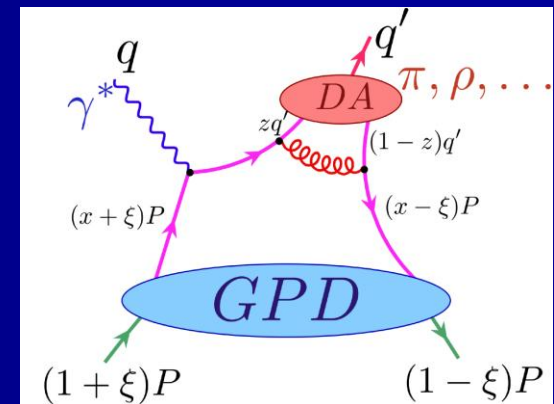
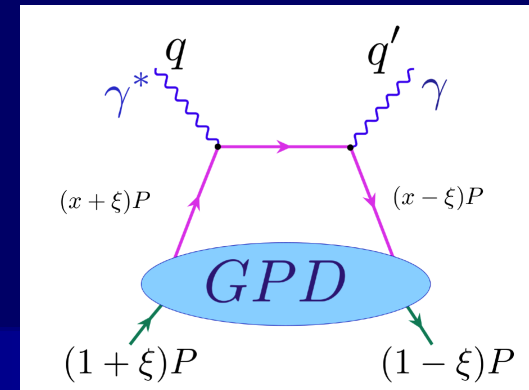
- Factorization theorem states that in the limit $Q^2 \rightarrow \infty$ exclusive electroproduction of mesons is described by hard rescattering amplitude, generalized parton distributions (GPDs), and the distribution amplitude $\Phi(z)$ of the outgoing meson.
- The prove applies only to the case when the virtual photon has **longitudinal polarization**
- $Q^2 \rightarrow \infty$ $\sigma_L \sim 1/Q^6$, $\sigma_T/\sigma_L \sim 1/Q^2$
- The full realization of this program is one of the major objectives of the 12 GeV upgrade

Deeply Virtual Meson production

$$ep \rightarrow ep\pi^0, \quad \pi^0 \rightarrow \gamma\gamma$$

$$ep \rightarrow ep\eta, \quad \eta \rightarrow \gamma\gamma$$

$$ep \rightarrow ep\rho^+, \quad \rho^+ \rightarrow \pi^+\pi^0$$



Meson	GPD flavor composition
π^+	$\Delta u - \Delta d$
π^0	$2\Delta u + \Delta d$
η	$2\Delta u - \Delta d$
ρ^0	$2u + d$
ρ^+	$u - d$
ω	$2u - d$

$$\tilde{H}, \tilde{E}$$

$$H, E$$

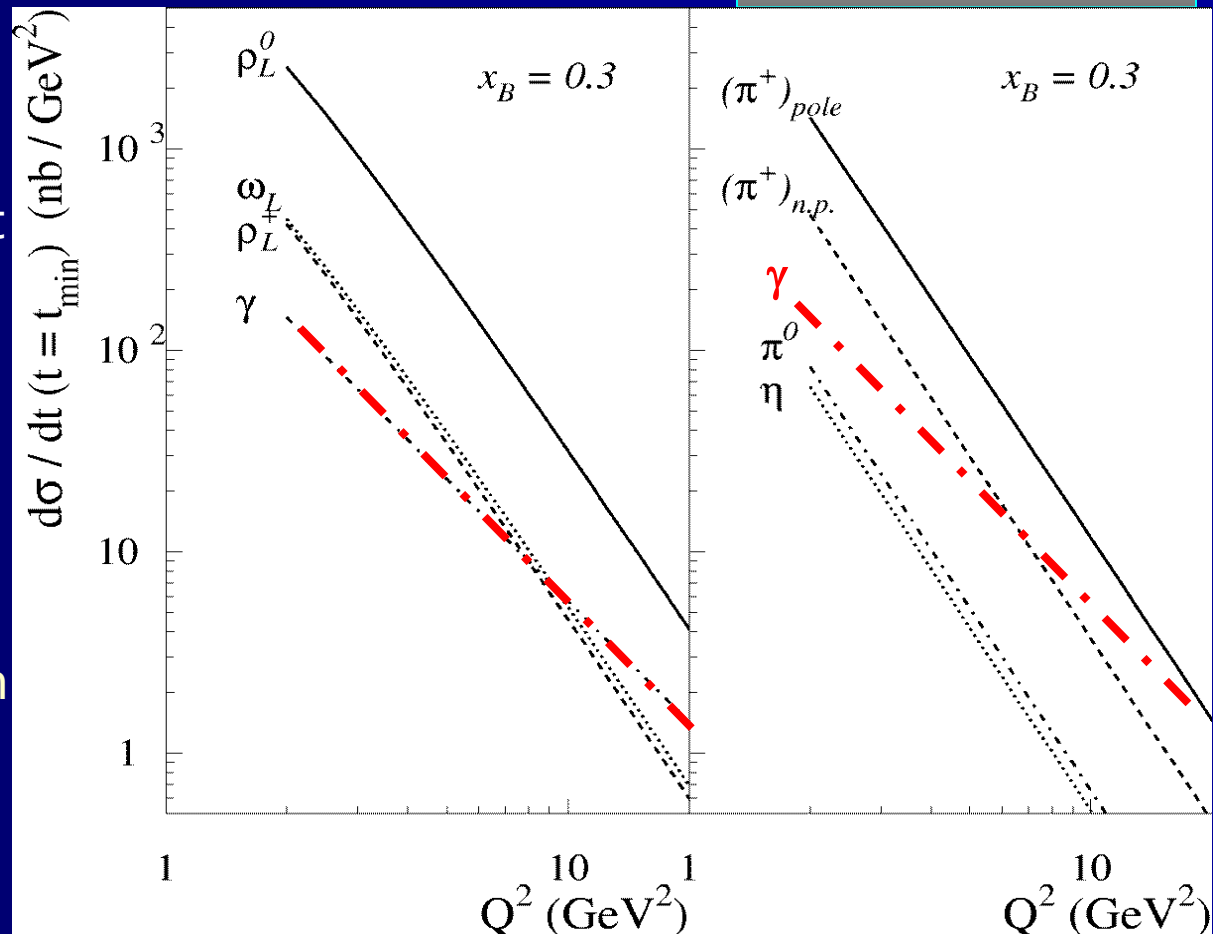
- DVCS is the cleanest way of accessing GPDs. However, it is difficult to perform a **flavor separation**.
- Vector and pseudoscalar meson production allows one to separate flavor and isolate the **helicity-dependent GPDs**.

GPD predictions (only σ_L)

Vanderhaeghen, Guichon, Guidal, 1999

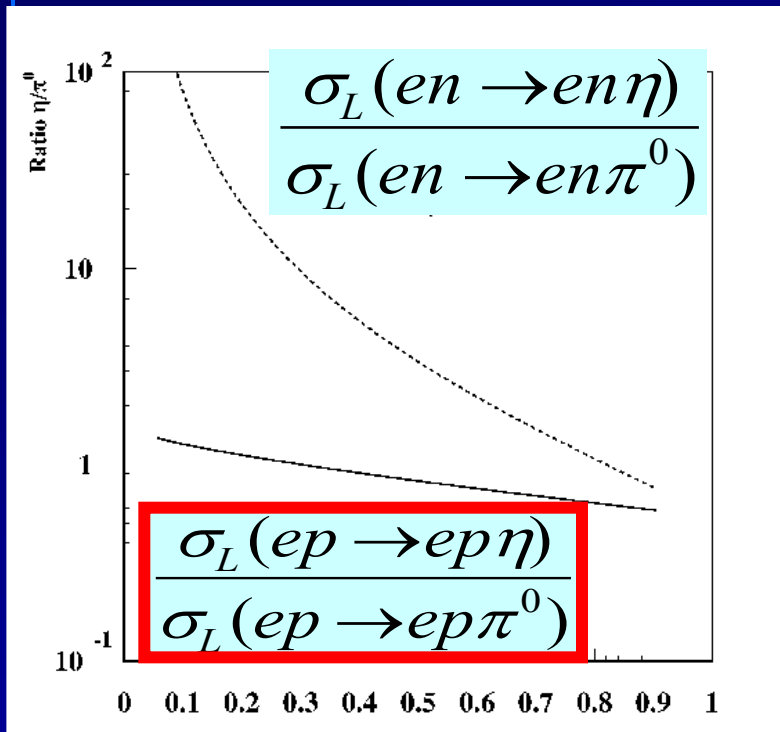
$$\frac{d\sigma_L}{dt} (t = t_{\min})$$

- $d\sigma_L/dt(t=t_{\min})$ for vector mesons (left panel)
- Pseudoscalar mesons (right panel)
- Note the pion pole contribution to the π^+ electroproduction (shown separately)
- The scaling cross section for photons dominate at high Q^2 over meson production.

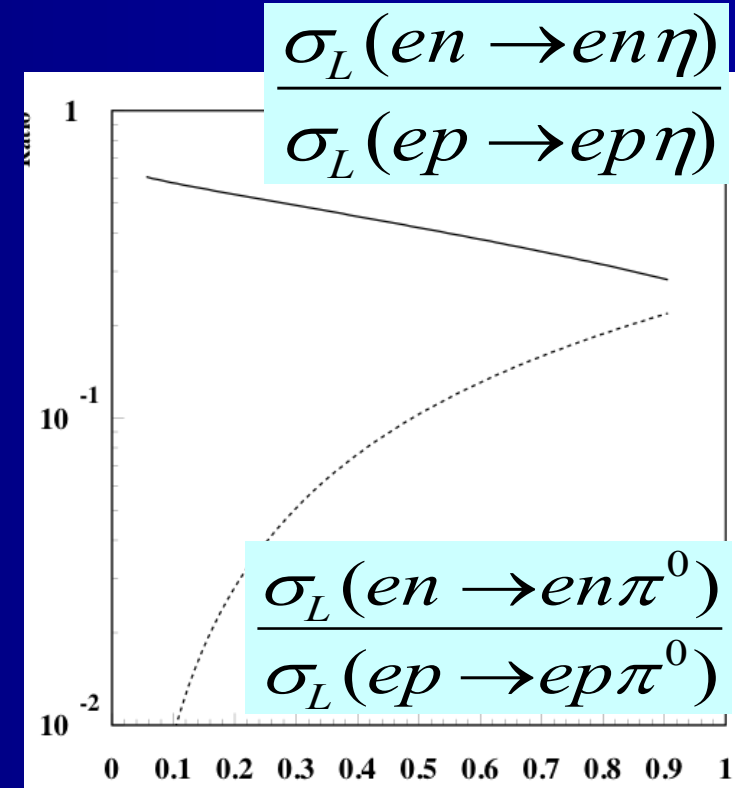


Cross Section Ratios as a function of x_B

Eides, Frankfurt, Strikman -1997



x_B



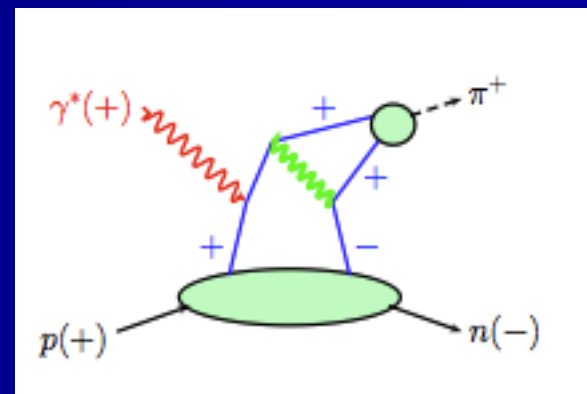
x_B

Transversity in DVMP

Kroll, Goloskokov
Goldstein, Luiti

- The data clearly show that a leading-twist calculation of DVMP within the handbag is insufficient. They demand higher-twist and/or power corrections.
- There is a large contribution from the helicity amplitude $M_{0-,++}$. Such contribution is generated by the the helicity-flip or transversity GPDs in combination with a twist-3 pion wave function.
- This explanation established an interesting connection to transversity parton distributions. The forward limit of H_T is the transversity distribution.

$$M_{0-,++} \sim H_T$$



$$H_T(x,0,0) = h_1(x)$$

π^0 electroproduction Handbag predictions

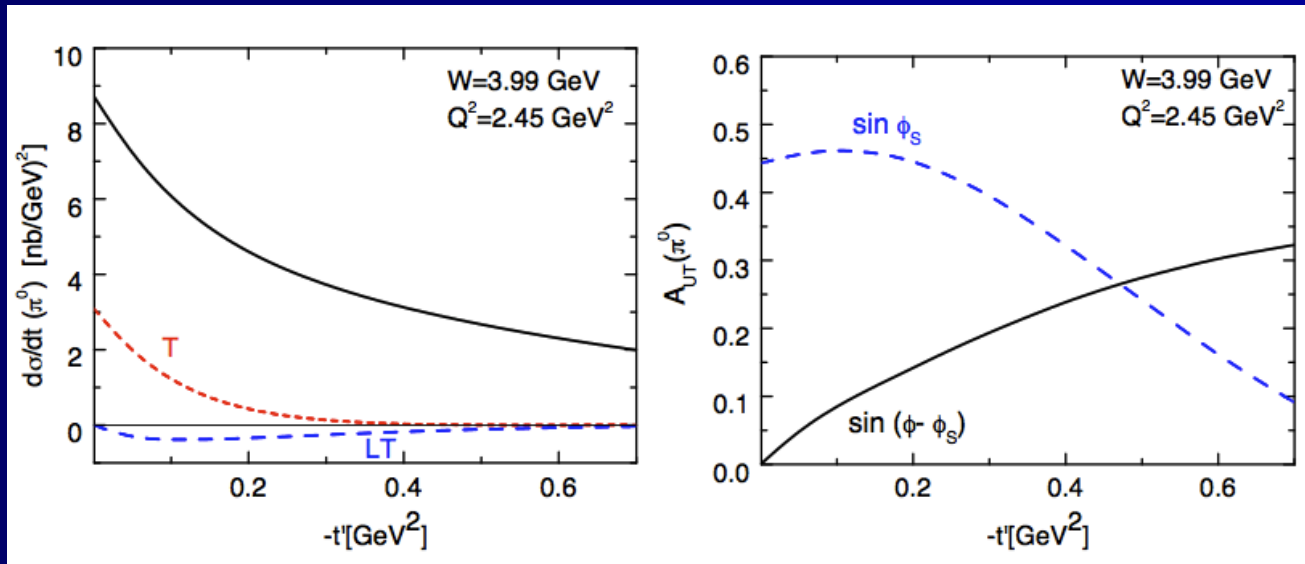
$$\gamma^* p \rightarrow p \pi^0$$

Kroll, Goloskokov, 2009.

$$\sigma_T + \epsilon \sigma_L$$

$$\sigma_T$$

$$\sigma_{LT}$$



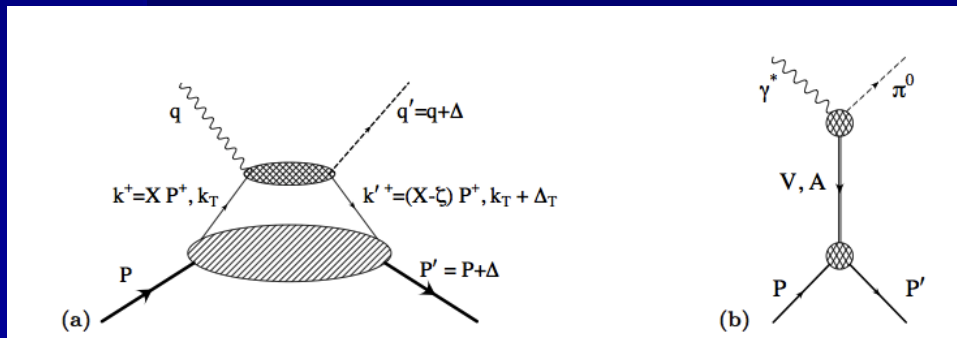
Predictions for the cross section (left) and A_{UT} (right) for the π^0 electroproduction versus $-t$. The unseparated (σ_L, σ_T) cross section was calculated as well as σ_T and σ_{LT} . At $W=2.2$ GeV the cross section will be a factor of 10 larger. We can check it at Jlab.

$$\gamma^* p \rightarrow p \pi^0$$

Nucleon Tensor Charge from Exclusive π^0 Electroproduction

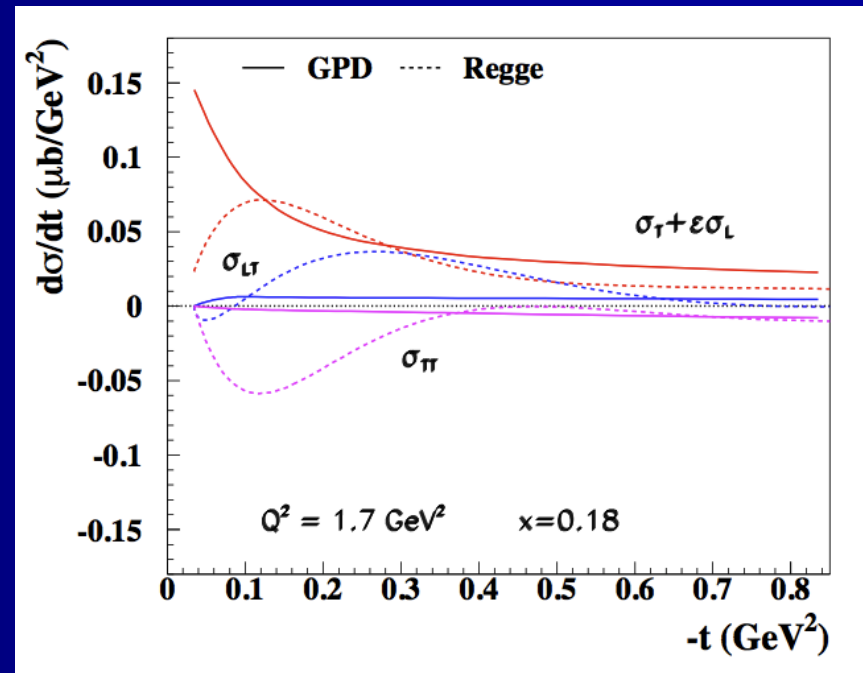
Ahmad, Goldstein, Luiti, 2009

- π^0 electroproduction proceeds through C-parity odd and chiral odd combination of t-channel exchange quantum numbers. This differs from DVCS and both vector and charge $\pi^{+/-}$ electroproduction, where the axial charge can enter the amplitudes.
- Contrary the tensor charge enters the π^0 process.



partonic degrees of freedom interpretation;

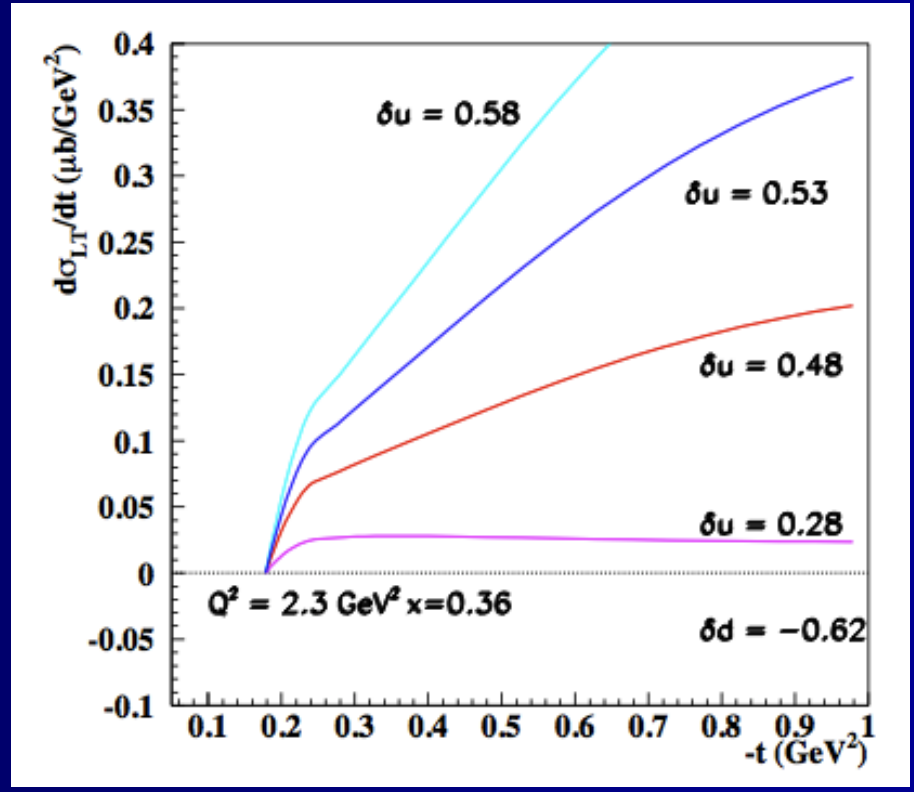
t-channel exchange diagram



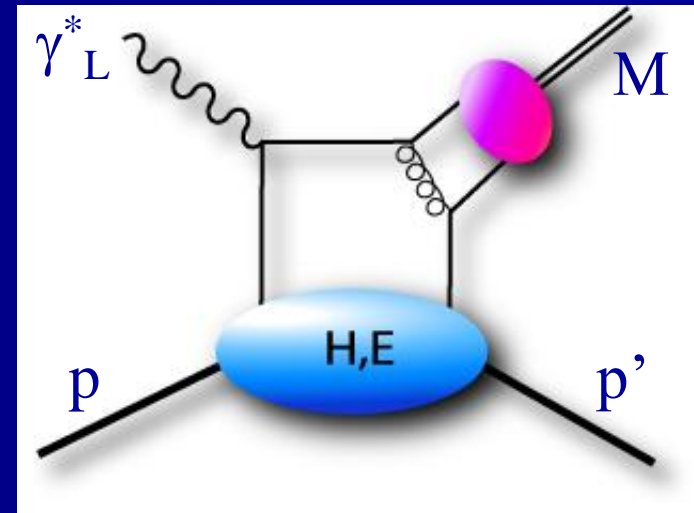
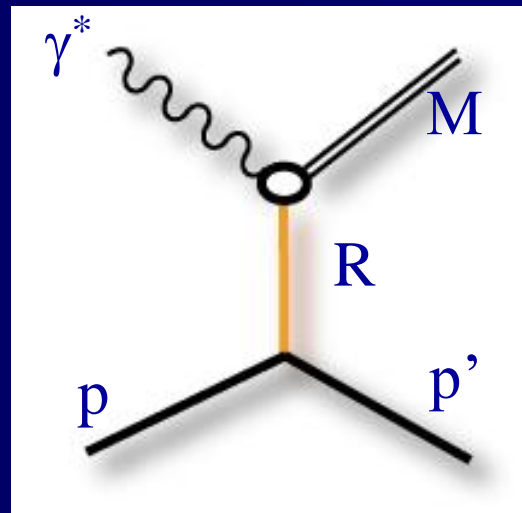
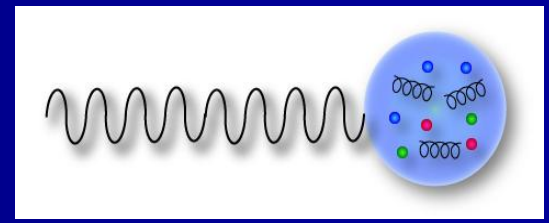
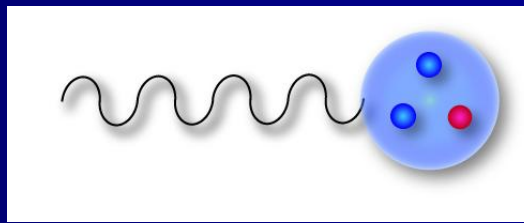
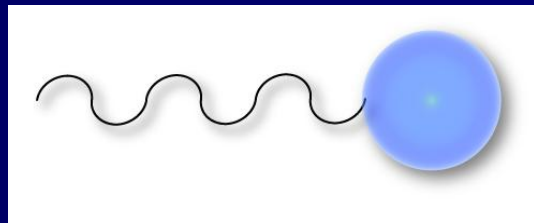
$$\gamma^* p \rightarrow p \pi^0$$

σ_{LT} for different values of the u quark tensor charge

Ahmad, Goldstein, Luiti, 2009



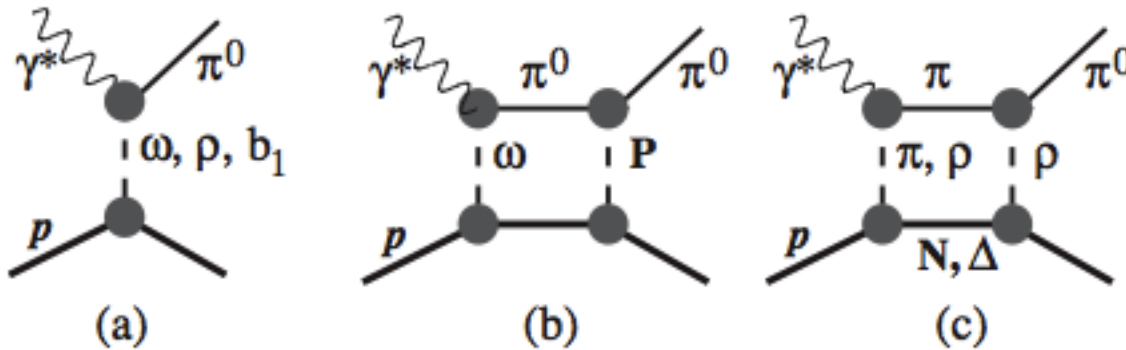
Transition from "hadronic" to the partonic degrees of freedom



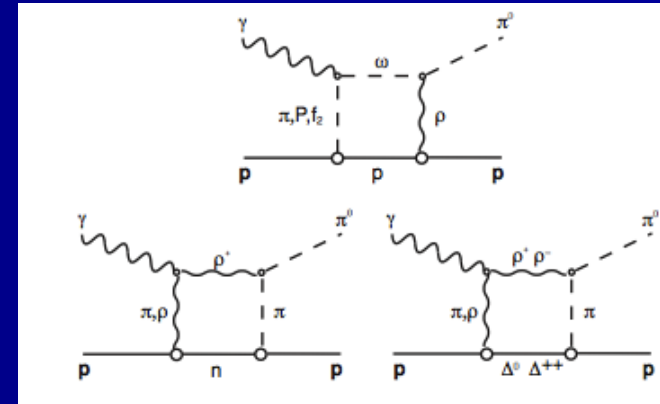
$$\gamma^* p \rightarrow p \pi^0$$

Regge Model

J.M. Laget 2010



- (a) Regge poles (vector and axial vector mesons)
- (b) and (c) pion cuts



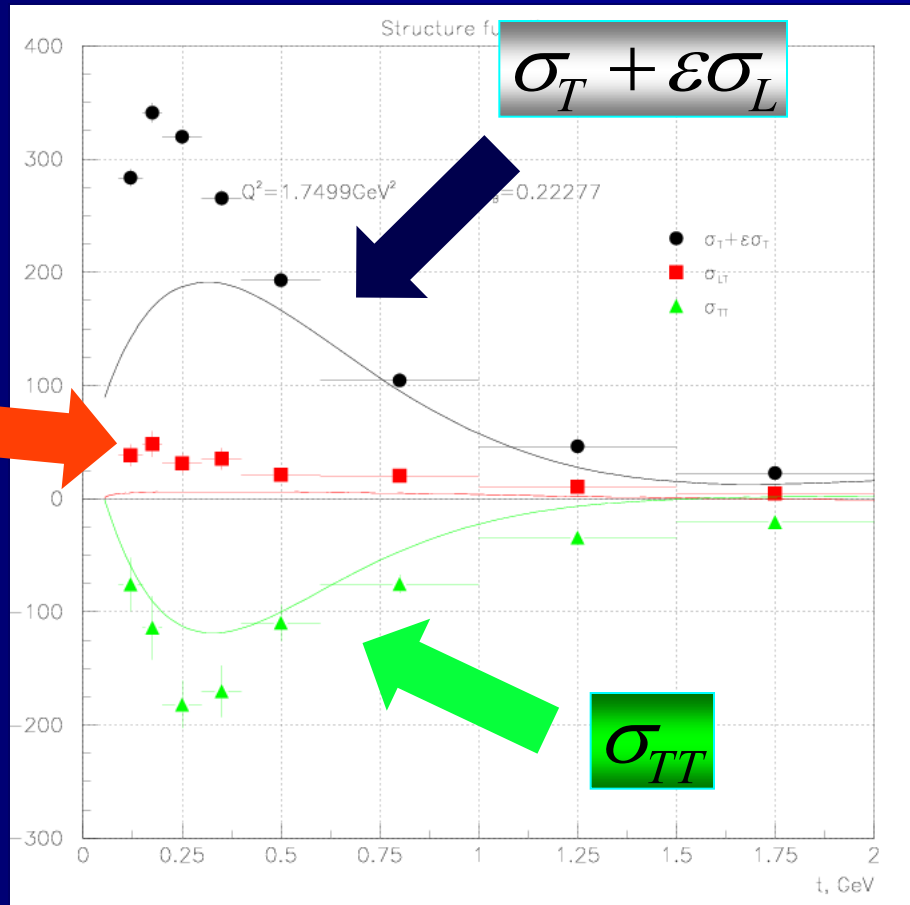
Vector meson cuts

$$\gamma^* p \rightarrow p \pi^0$$

Regge predictions

$Q^2=1.75$
 $x^B=0.22$

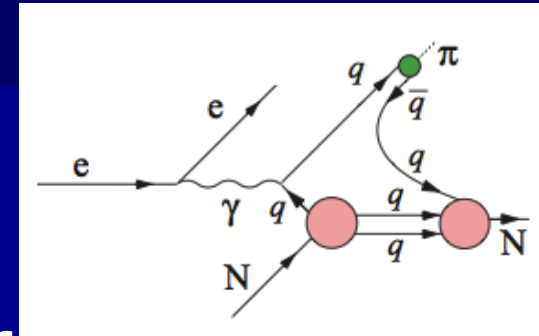
σ_{LT}



-t, GeV²

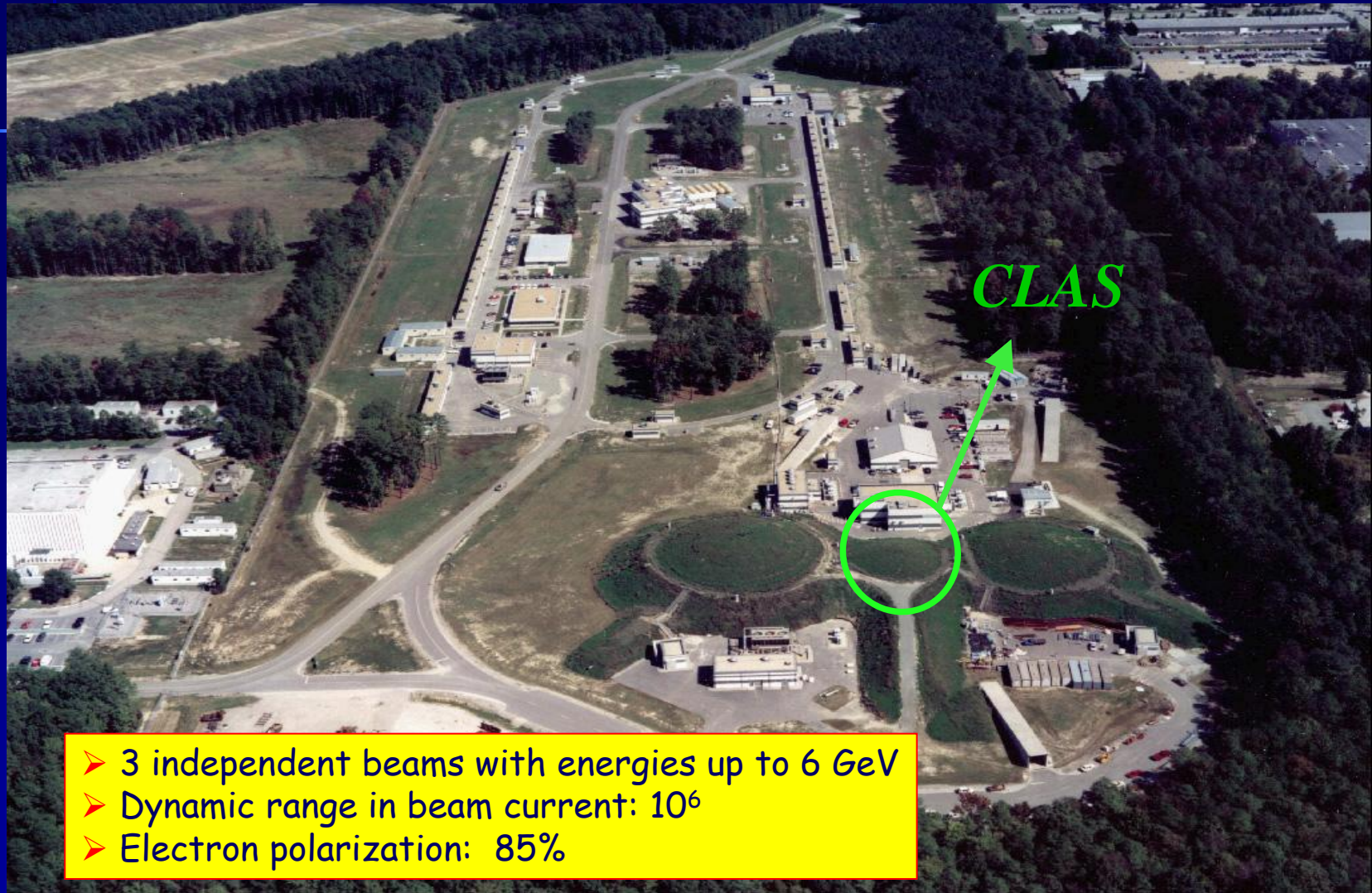
Combined Regge + DIS model

Kaskulov, Gallmeister, Mosel (2008-2010)



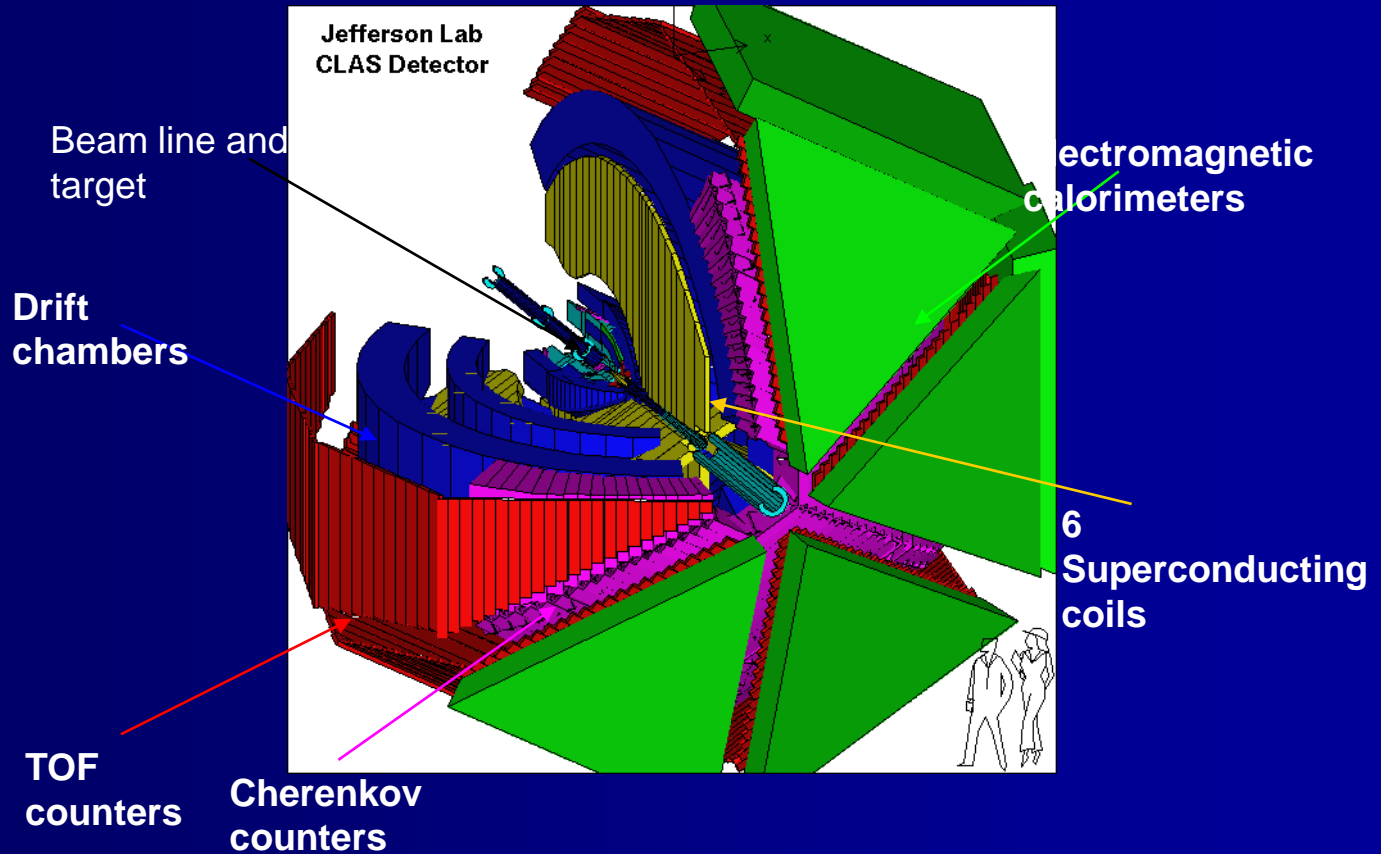
- σ_L is dominated by improved treatment of gauge Invariant Regge model.
- σ_T is described by direct hard interaction of virtual photons with partons followed by the hadronization process into πN channel.
- This explains the large transverse response at moderate and high photon virtualities.
- This process is sensitive to the intrinsic transverse momentum distribution of partons.

JLab Site: The 6 GeV Electron Accelerator



- 3 independent beams with energies up to 6 GeV
- Dynamic range in beam current: 10^6
- Electron polarization: 85%

CEBAF Large Acceptance Spectrometer CLAS



CLAS (forward carriage and side clamshells retracted)

Large angle EC

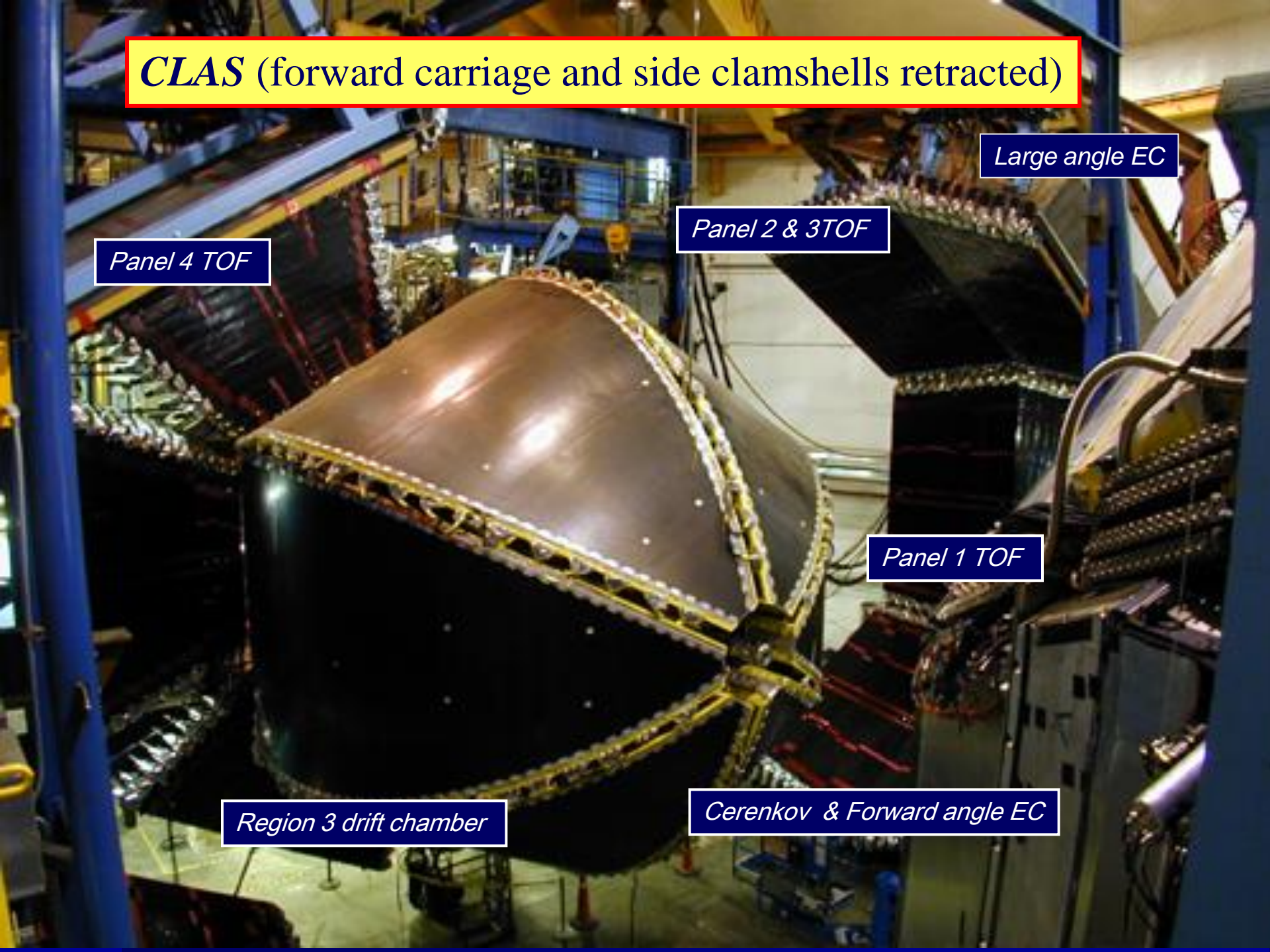
Panel 2 & 3 TOF

Panel 4 TOF

Panel 1 TOF

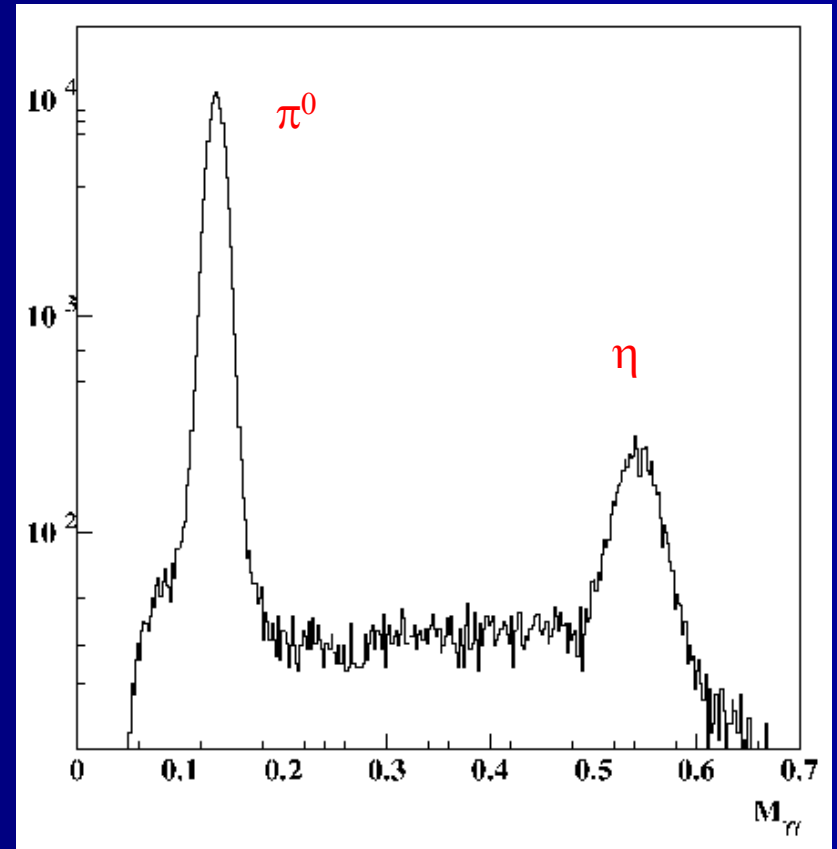
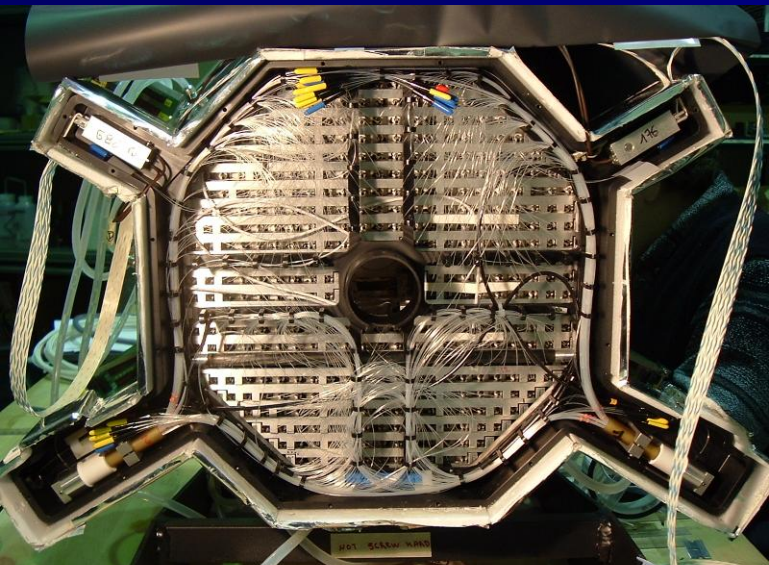
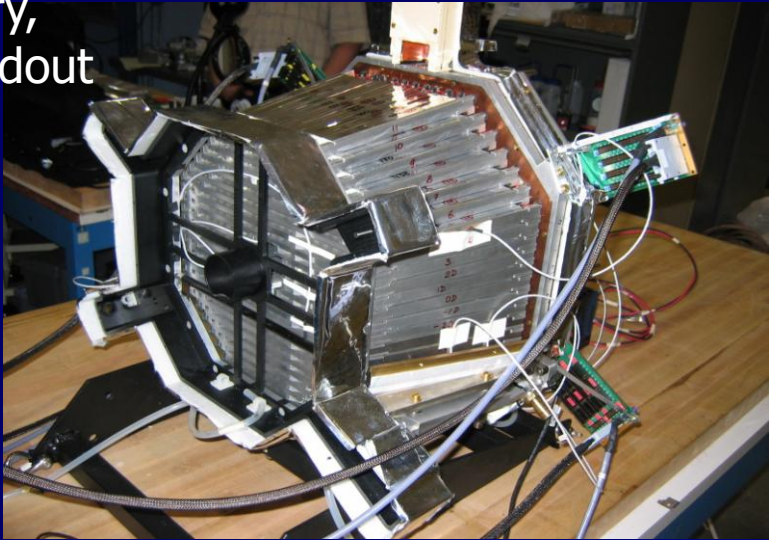
Region 3 drift chamber

Cerenkov & Forward angle EC



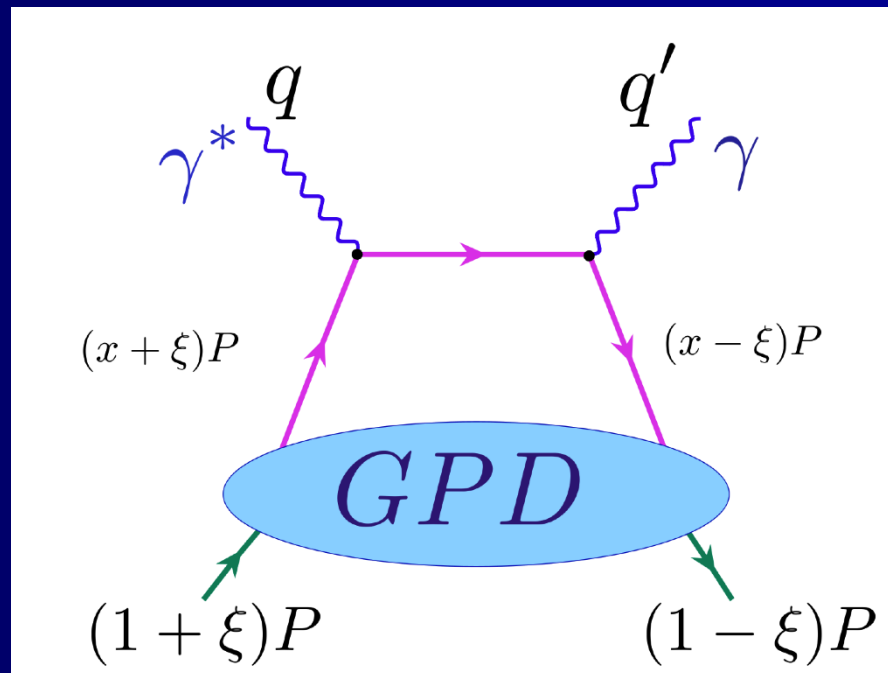
CLAS Lead Tungstate Electromagnetic Calorimeter

424 crystals,
18 RL,
pointing
geometry,
APD readout



Deeply Virtual Compton Scattering

The cleanest process to access GPDs



DVCS BSA A_{LU}

$$A_{LU} = \frac{\sigma^+ - \sigma^-}{\sigma^+ + \sigma^-} = \frac{\Delta\sigma}{2\sigma}$$

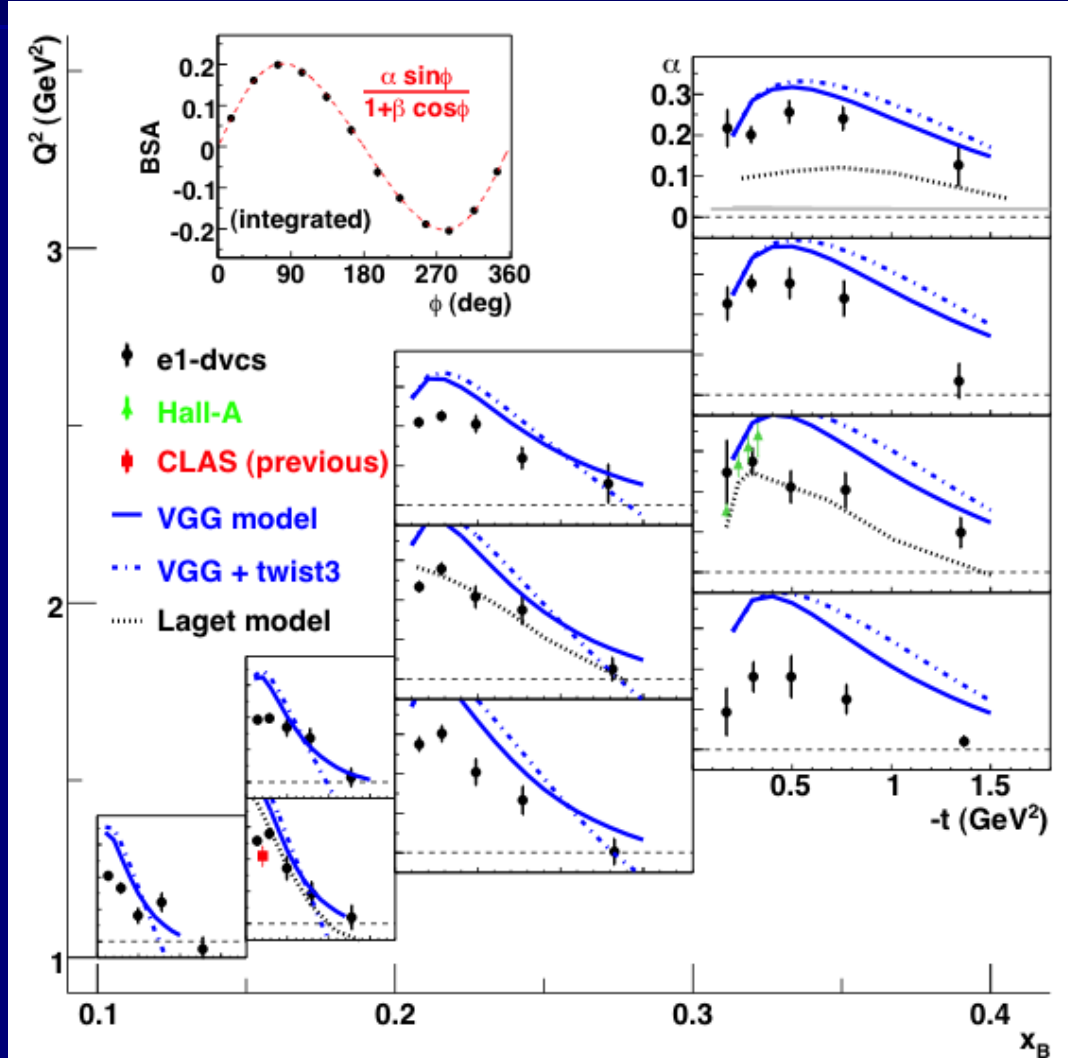
$$\text{Fit: } A_{LU} = \alpha \sin\phi / (1 + \beta \cos\phi)$$

$$\Delta\sigma_{LU} \sim \sin\phi \{F_1 H + \xi(F_1 + F_2) \tilde{H} + \dots\} d\phi$$

VGG parameterization reproduces $-t > 0.5 \text{ GeV}^2$ behavior, and overshoots asymmetry at small t .

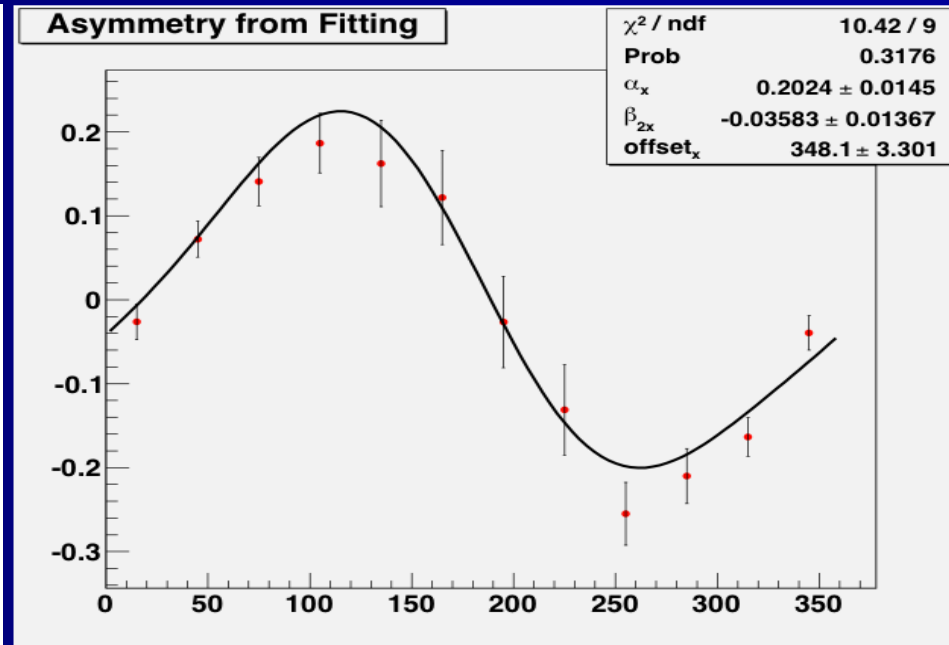
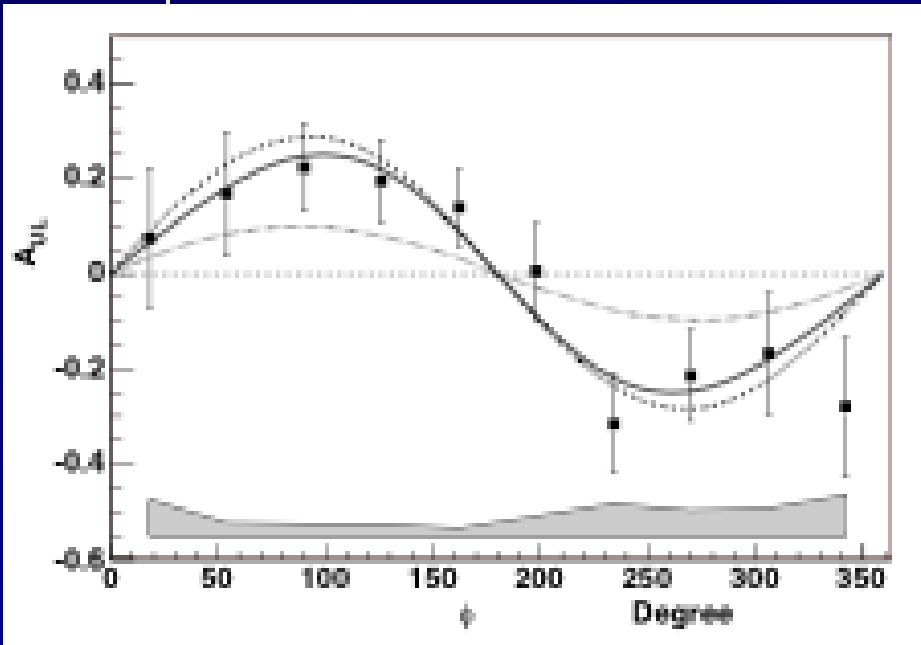
Regge model (J-M Laget) is in fair agreement in some kinematic bins with our results.

Phys.Rev.Lett 100:162002, 2008



Target Spin Asymmetry A_{UL}

(new data taken @2010)

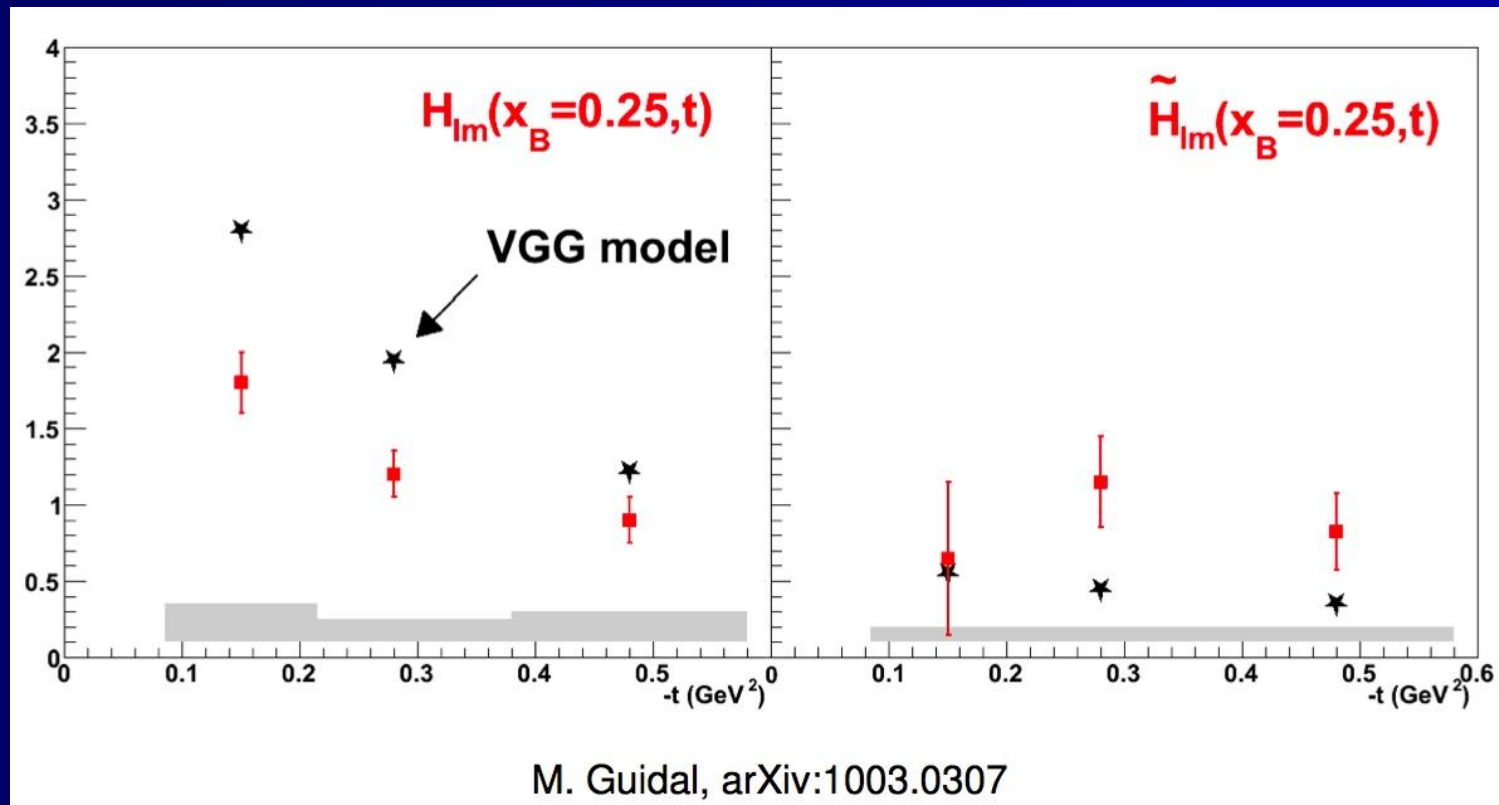


Phys.Rev.Lett 97:072002, 2006

eg1-dvcs (2010), not full statistics

Extraction of Compton Form Factors from CLAS DVCS data

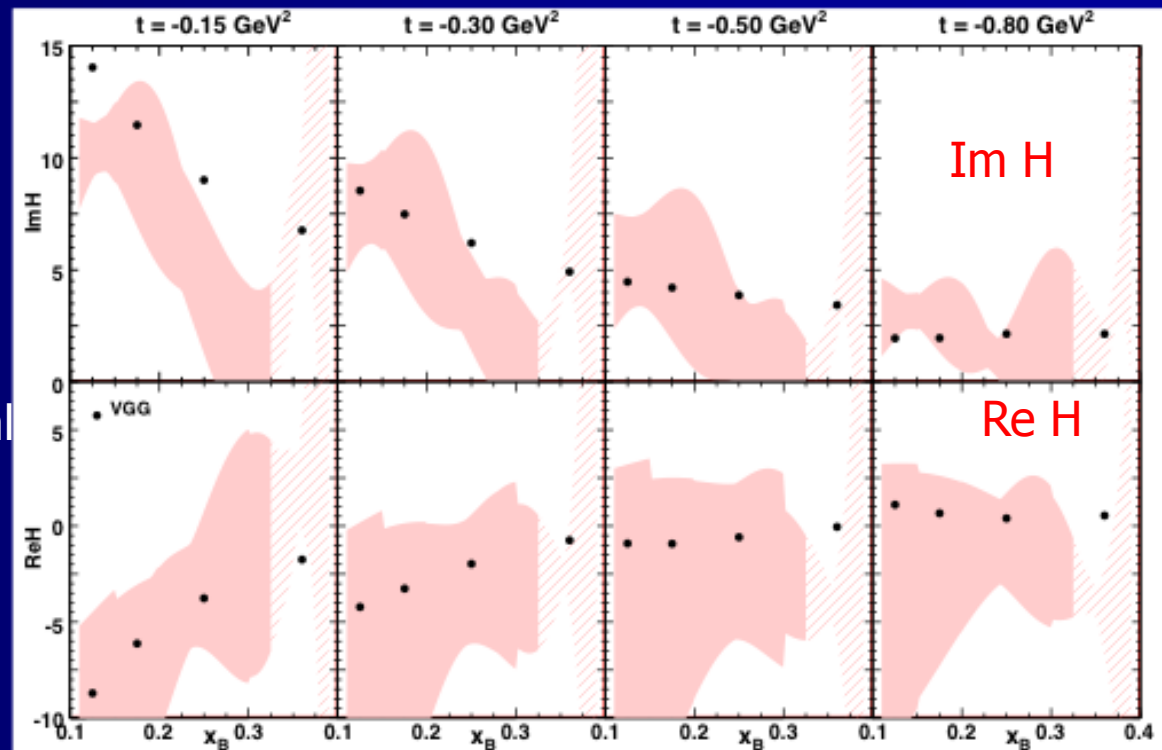
- A_{LU} and A_{UL} \tilde{H} CLAS results only
- $Im H(t)$ more flat than $Im \tilde{H}(t)$



Global Analysis of the Compton FF (Jlab data)

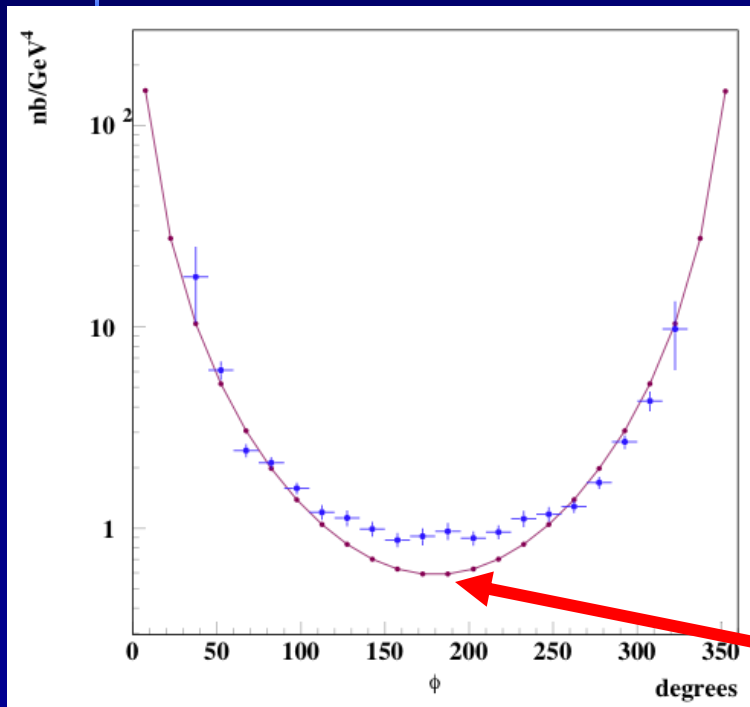
$$CFF = \int_{-1}^{+1} F(x, \xi, t) \left(\frac{1}{\xi - x - i\varepsilon} \pm \frac{1}{\xi + x - i\varepsilon} \right) dx$$

- The points are VGG model prediction
- The shadow is the Real and Imaginary parts of the CFF extracted from the experimental data

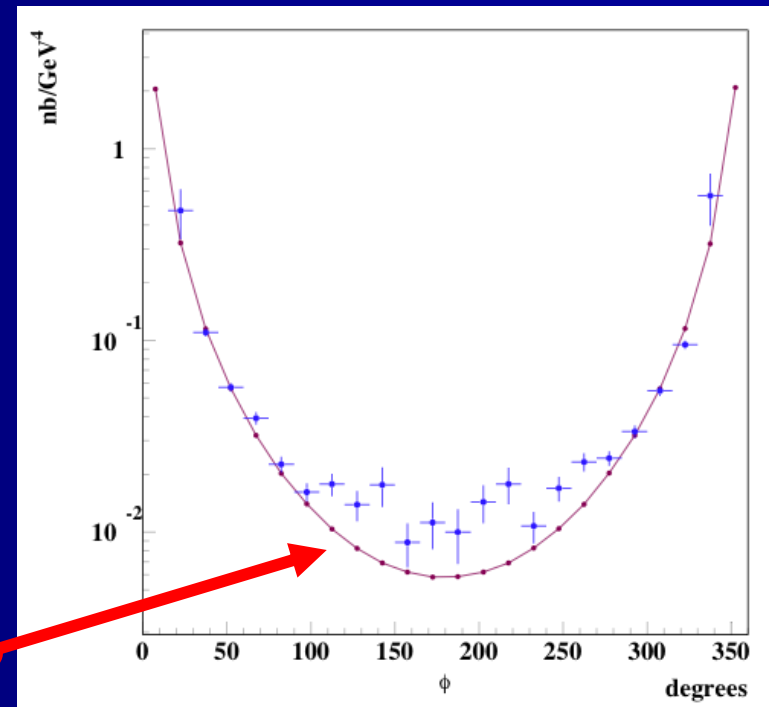


DVCS cross section

preliminary



$Q^2=1.2 \text{ GeV}^2$ $x_B=0.13$ $t=0.12 \text{ GeV}^2$



$Q^2=2.2 \text{ GeV}^2$ $x_B=0.25$ $t=0.45 \text{ GeV}^2$

BH

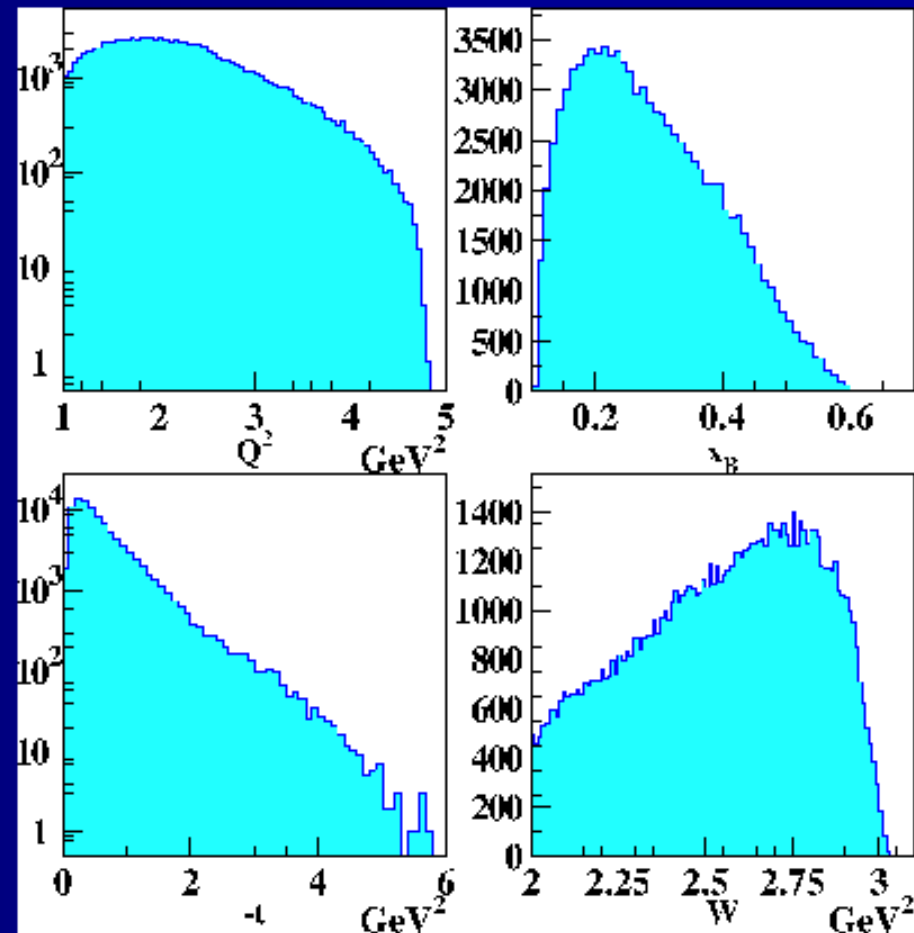
DVMP: Kinematic Coverage

4 dimensional grid in Q^2 , x_B , t , and ϕ

$$ep \rightarrow ep\pi^0, \quad \pi^0 \rightarrow \gamma\gamma$$

$$ep \rightarrow ep\eta, \quad \eta \rightarrow \gamma\gamma$$

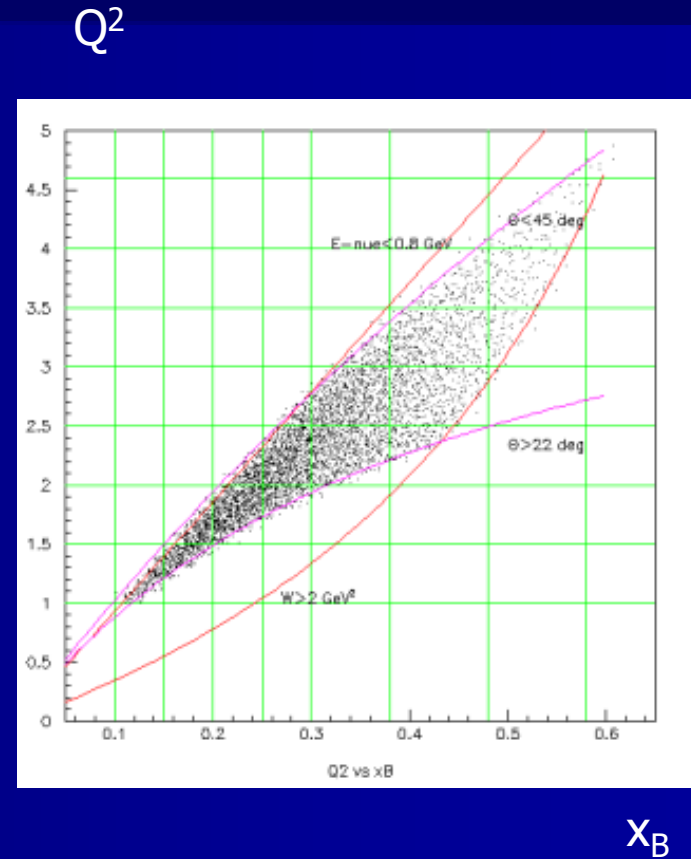
- Polarized Electron Beam
- $E_0 = 5.776$ GeV
- 75-80% polarization
- 2.5 cm Liquid Hydrogen target
- IC calorimeter
- Instant luminosity $2 \cdot 10^{34} \text{ cm}^{-2}\text{s}^{-1}$
- Integrated luminosity: $3.27 \cdot 10^7 \text{ nb}^{-1}$



4 Dimensional Grid

Rectangular bins are used.

- Q^2 - 7 bins(1.-4.5 GeV^2)
- x_B - 7 bins(0.1-0.58)
- t - 8 bins(0.09-2.0 GeV)
- ϕ - 20 bins(0-360 $^\circ$)
- π^0 data ~ 2000 points
- η data ~ 1000 points



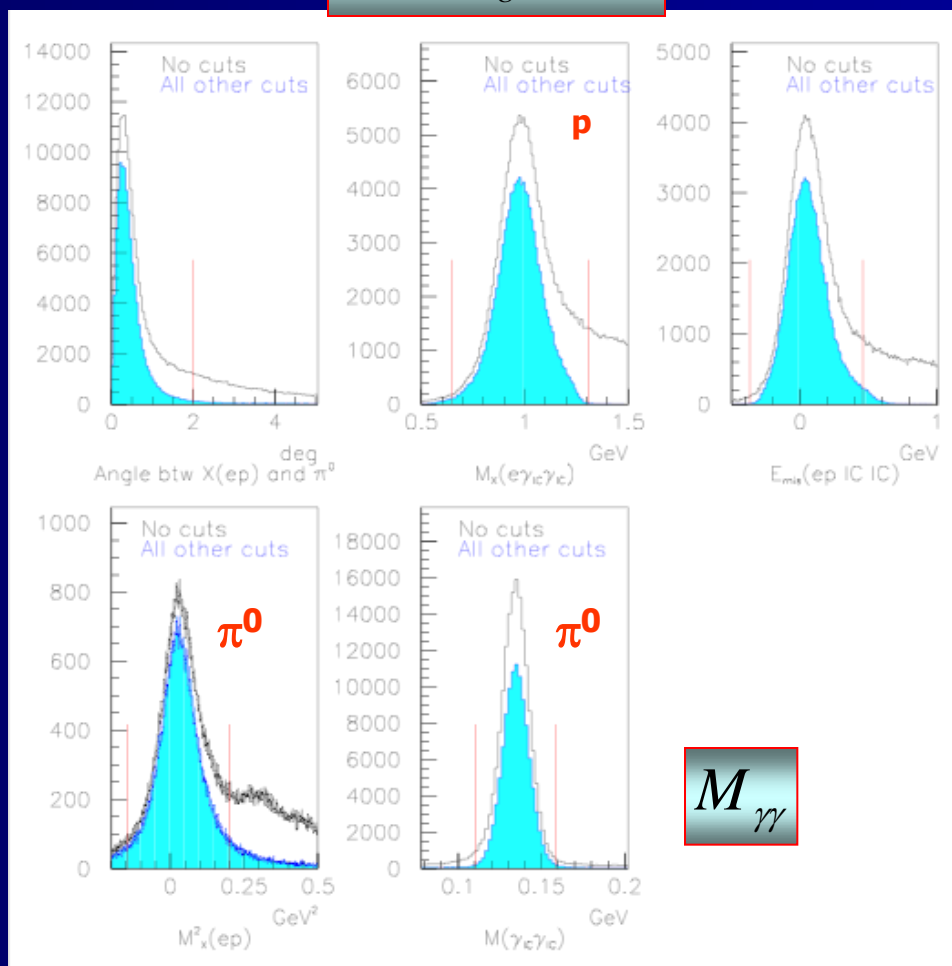
Exclusivity Cuts

$$ep \rightarrow ep\pi^0, \quad \pi^0 \rightarrow \gamma\gamma$$

$$M_{\text{missing}}(e\gamma\gamma)$$

$$\theta(X_{\text{missing}}^{ep}, \gamma\gamma)$$

$$E_{\text{missing}}$$



$$M_{\gamma\gamma}$$

$$M_{\text{missing}}^2(ep)$$

Monte Carlo

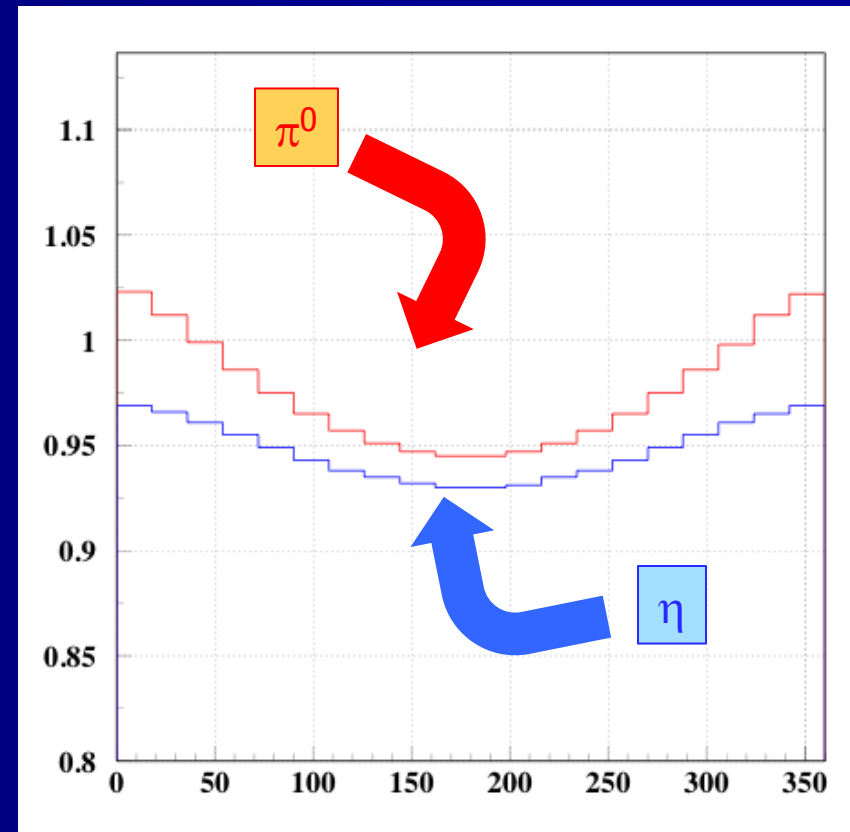
- Empirical model for the structure cross sections was used for the MC simulation and radiative corrections
- This model is based on CLAS data
- MC simulation included the radiative effects and used empirical model for the Born term.
- 100 M events were simulated with GSIM program.

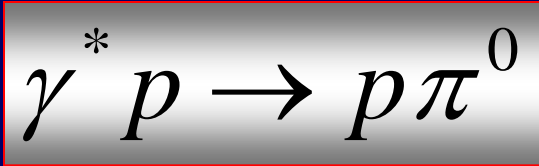
Radiative Corrections

- Radiative Corrections were calculated using **Exclurad** package adapted by Kyungseon with structure cross sections described by our empirical cross section.

$$Q^2 = 1.15 \text{ GeV}^2 \quad x_B = 0.13 \quad -t = 0.1 \text{ GeV}^2$$

$$RadCor = \frac{\sigma_{Rad}}{\sigma_{Born}}$$

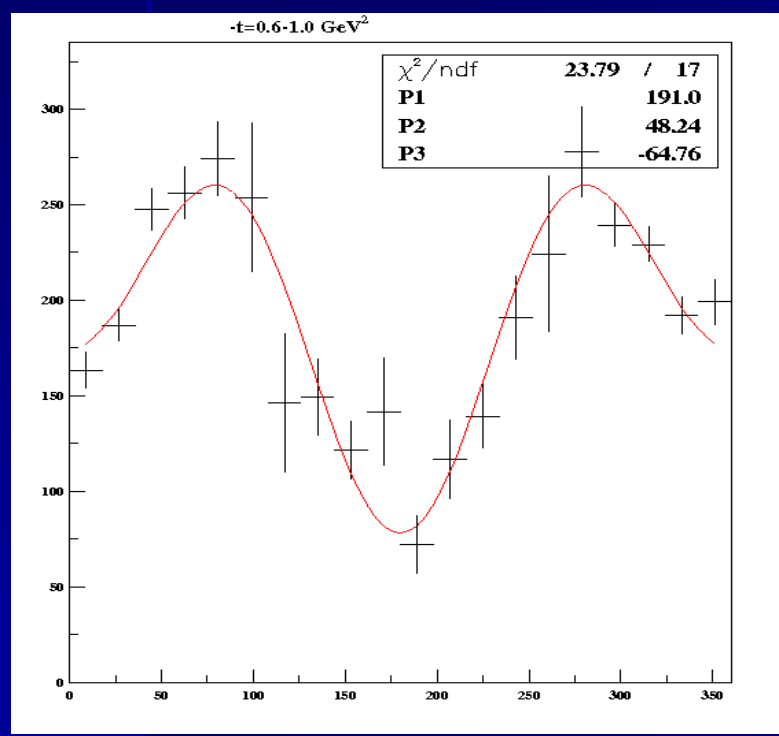




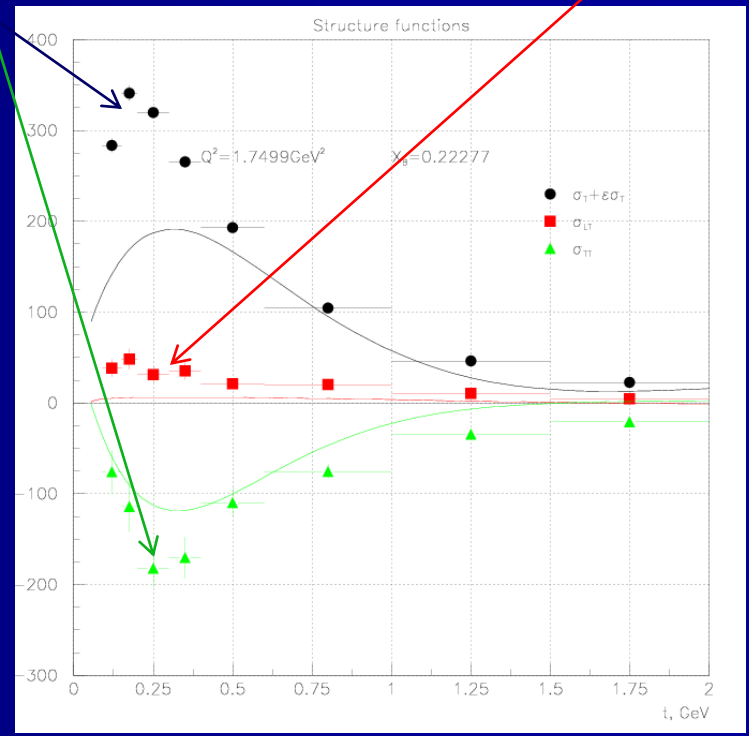
Structure Functions

$\sigma_T + \varepsilon \sigma_L$ σ_{TT} σ_{LT}

$$\frac{d\sigma}{dt d\phi}(Q^2, x, t, \phi) = \frac{1}{2\pi} \left(\frac{d\sigma_T}{dt} + \varepsilon \frac{d\sigma_L}{dt} \right) + \varepsilon \frac{d\sigma_{TT}}{dt} \cos 2\phi + \sqrt{2\varepsilon(\varepsilon+1)} \frac{d\sigma_{LT}}{dt} \cos \phi$$



ϕ distribution

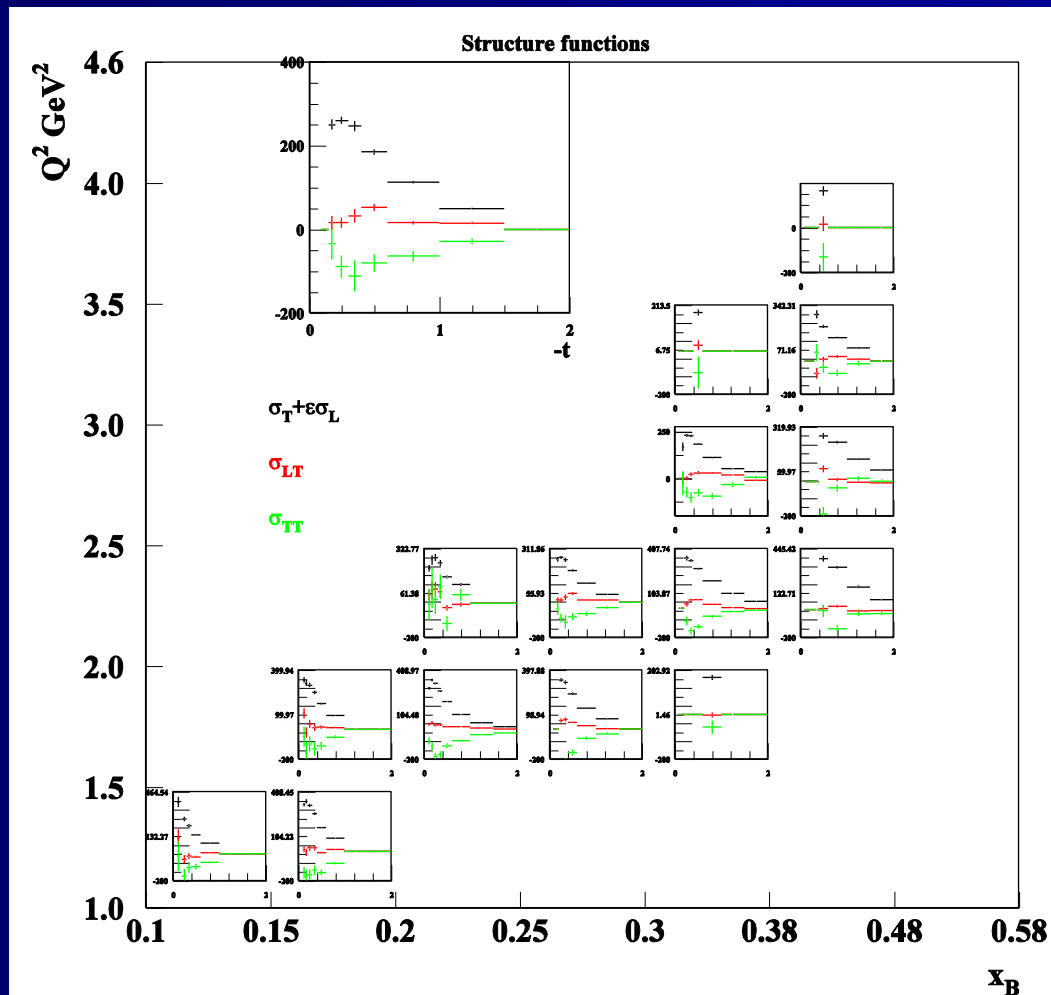


GM Laget Regge model

Structure Functions

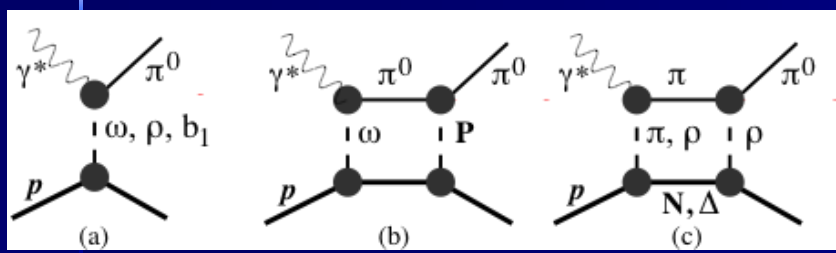
$(\sigma_T + \varepsilon\sigma_L)$ σ_{TT} σ_{LT}

$$\gamma^* p \rightarrow p \pi^0$$



$$\gamma^* p \rightarrow p \pi^0$$

$(\sigma_T + \epsilon\sigma_L)$ σ_{TT} σ_{LT} in Regge Model (J-M Laget)

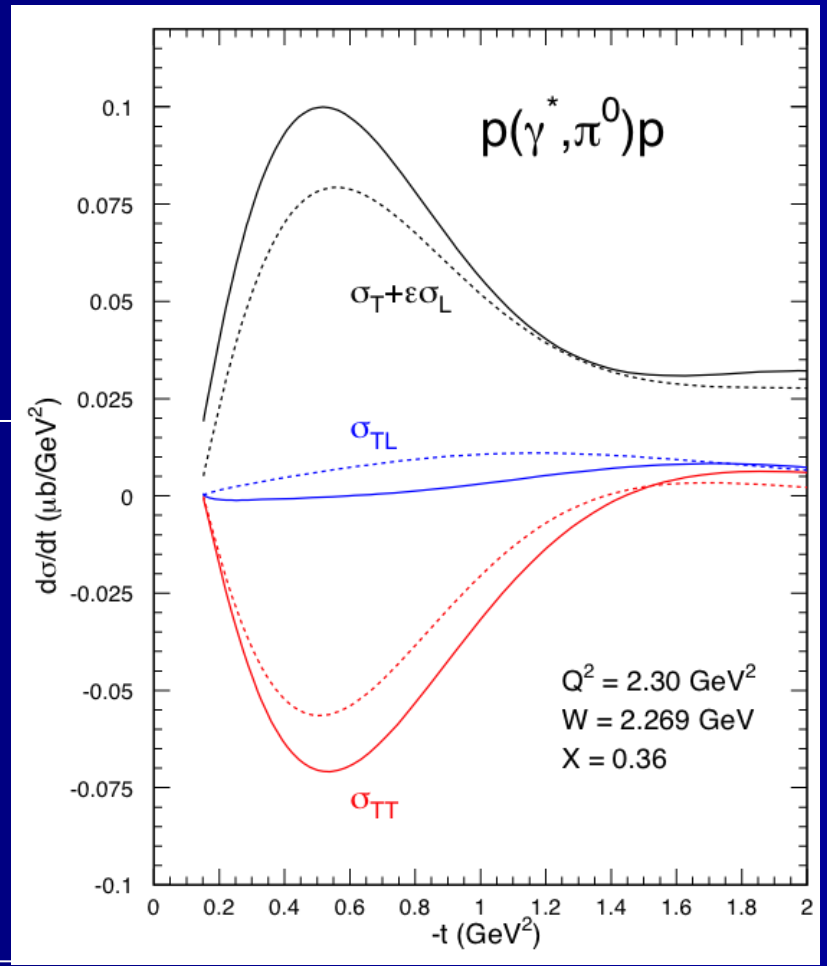


$\omega/\rho/b_1$

elastic rescat.

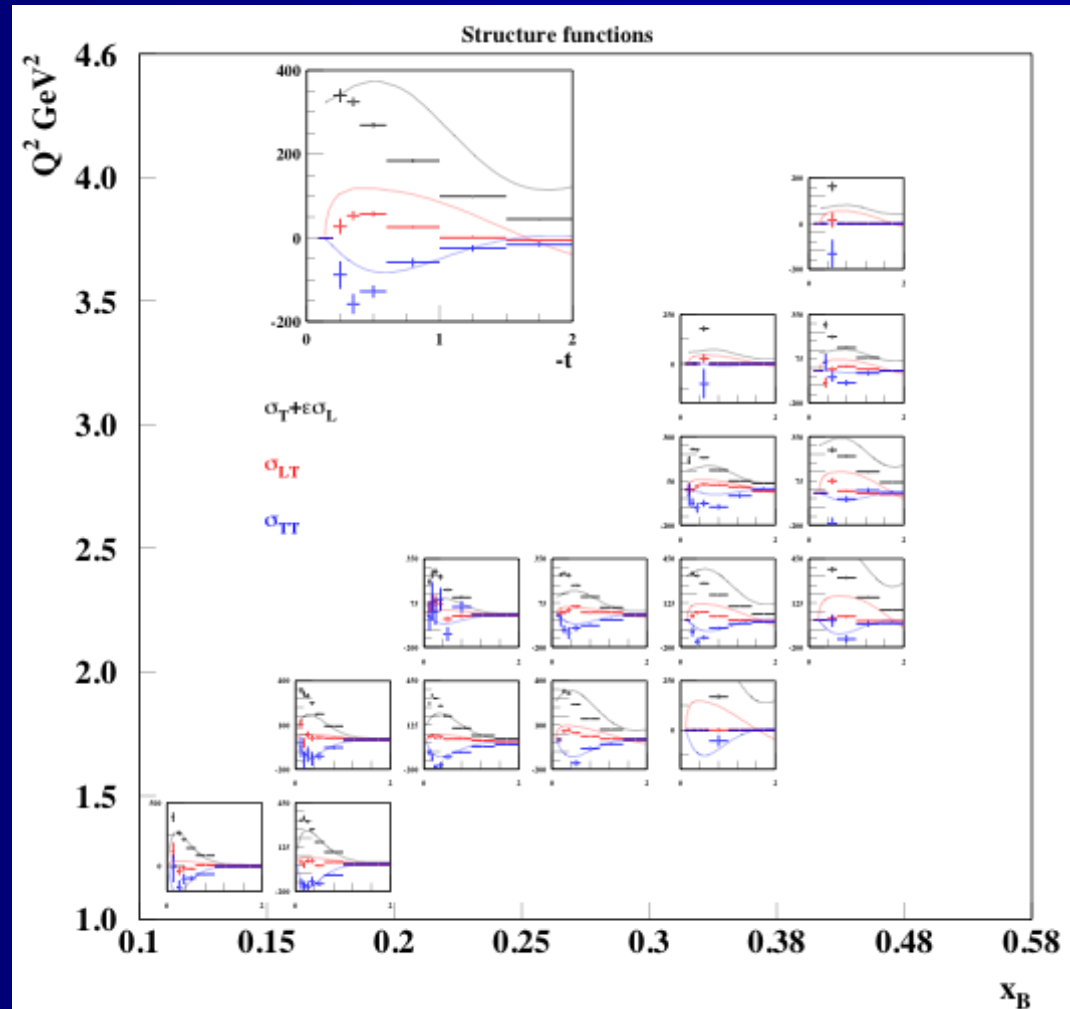
charge pion

- The dashed lines correspond to the $\omega/\rho/b_1$ Regge poles and elastic rescattering
- The full lines include also charge pion nucleon and Delta intermediate states.
- Regge model qualitatively describes the experimental data

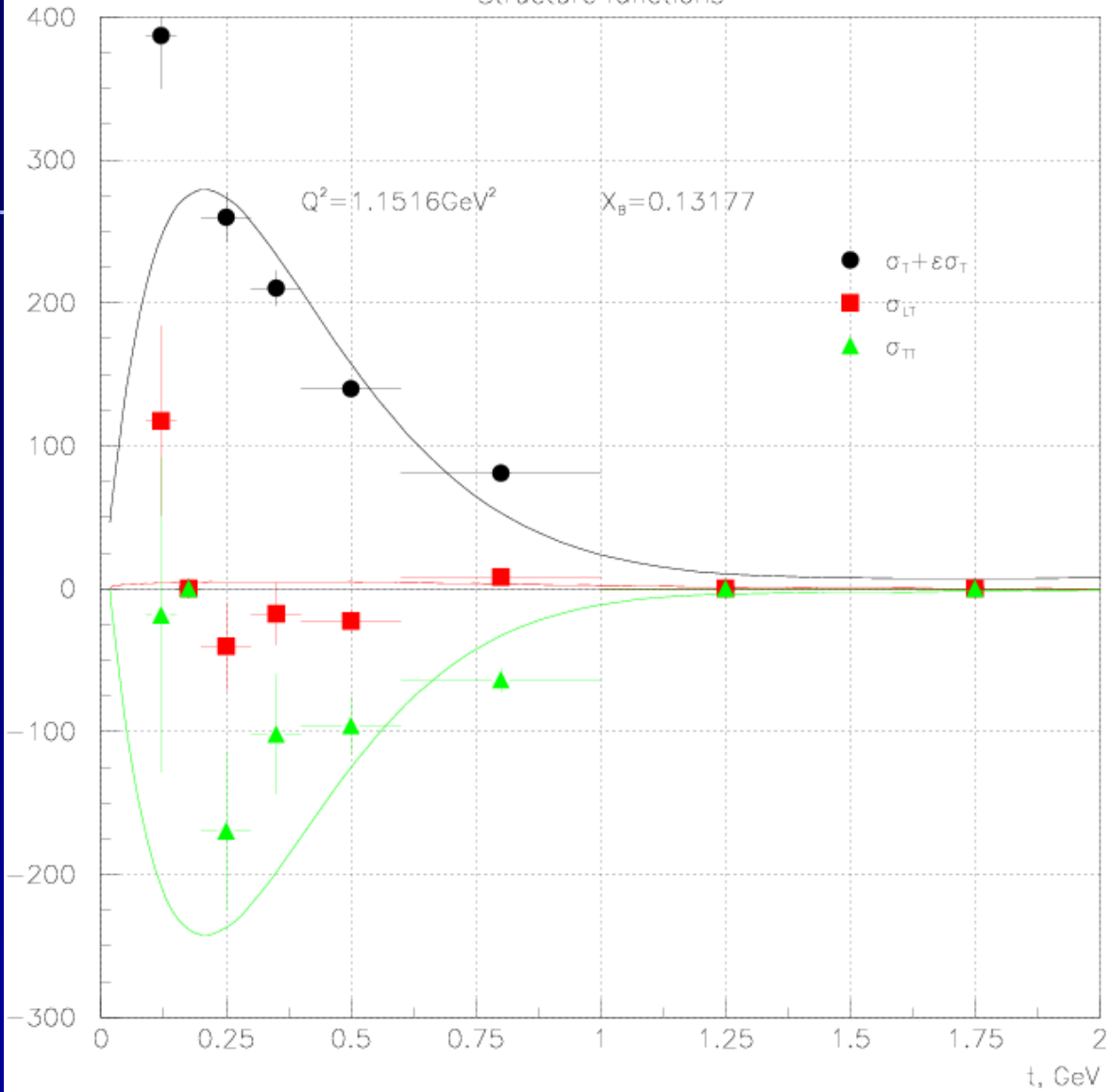


Comparison with J.M. Laget Regge model

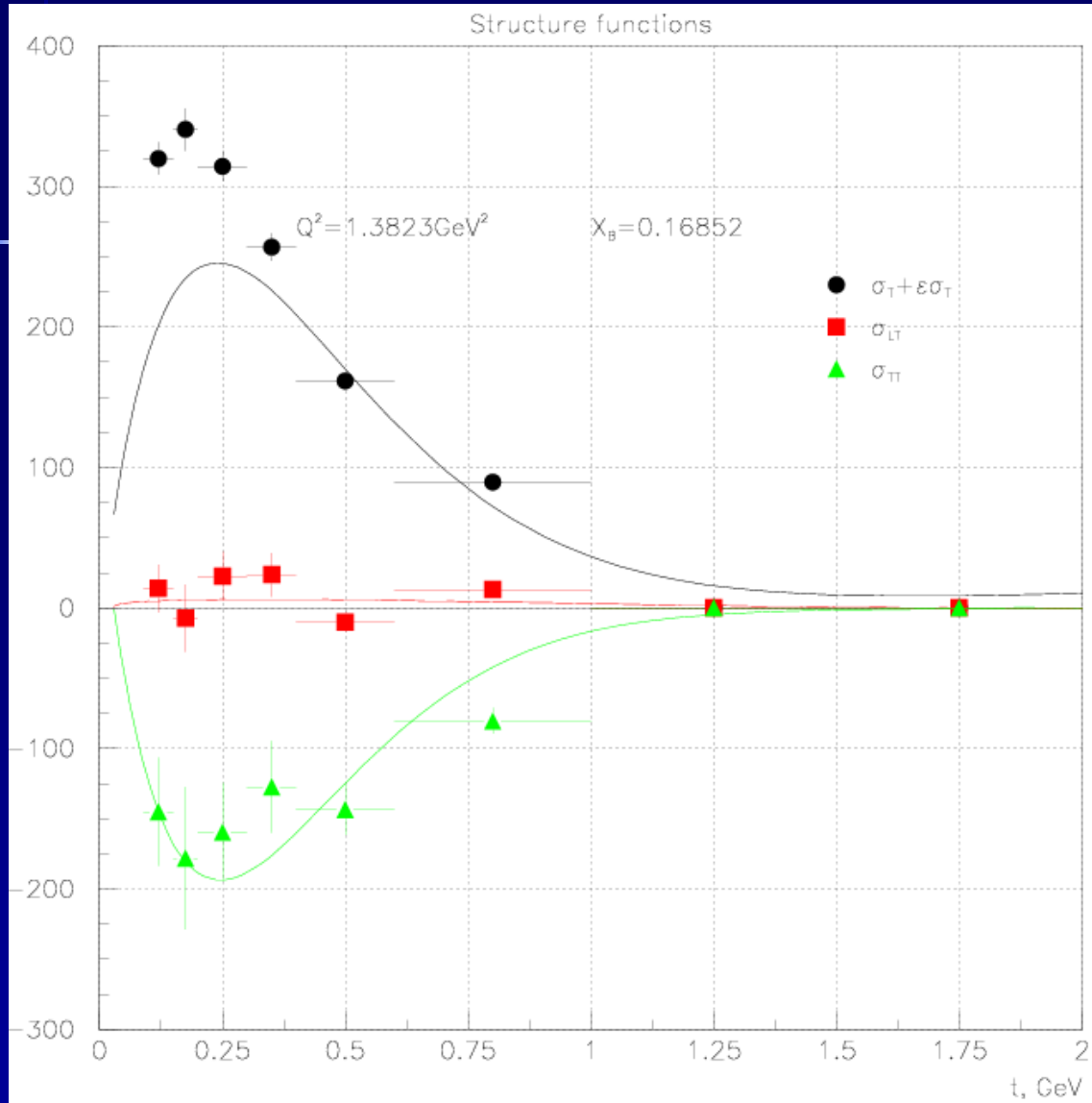
- Extracted reduced cross sections were compared with predictions of J.M. Laget Regge Model



Structure functions

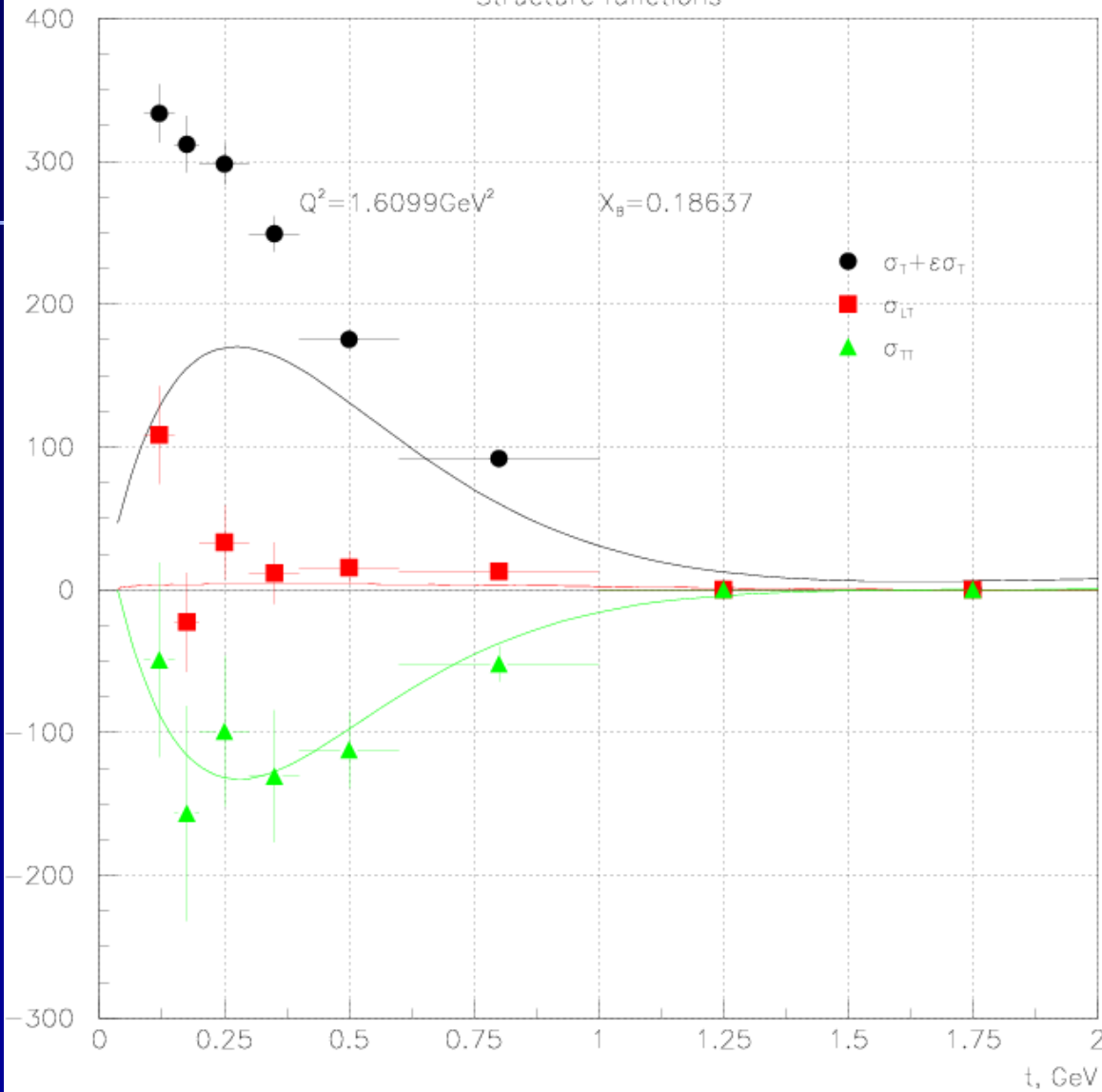


$Q^2 = 1.15 \text{ GeV}^2$
 $X_B = 0.13$



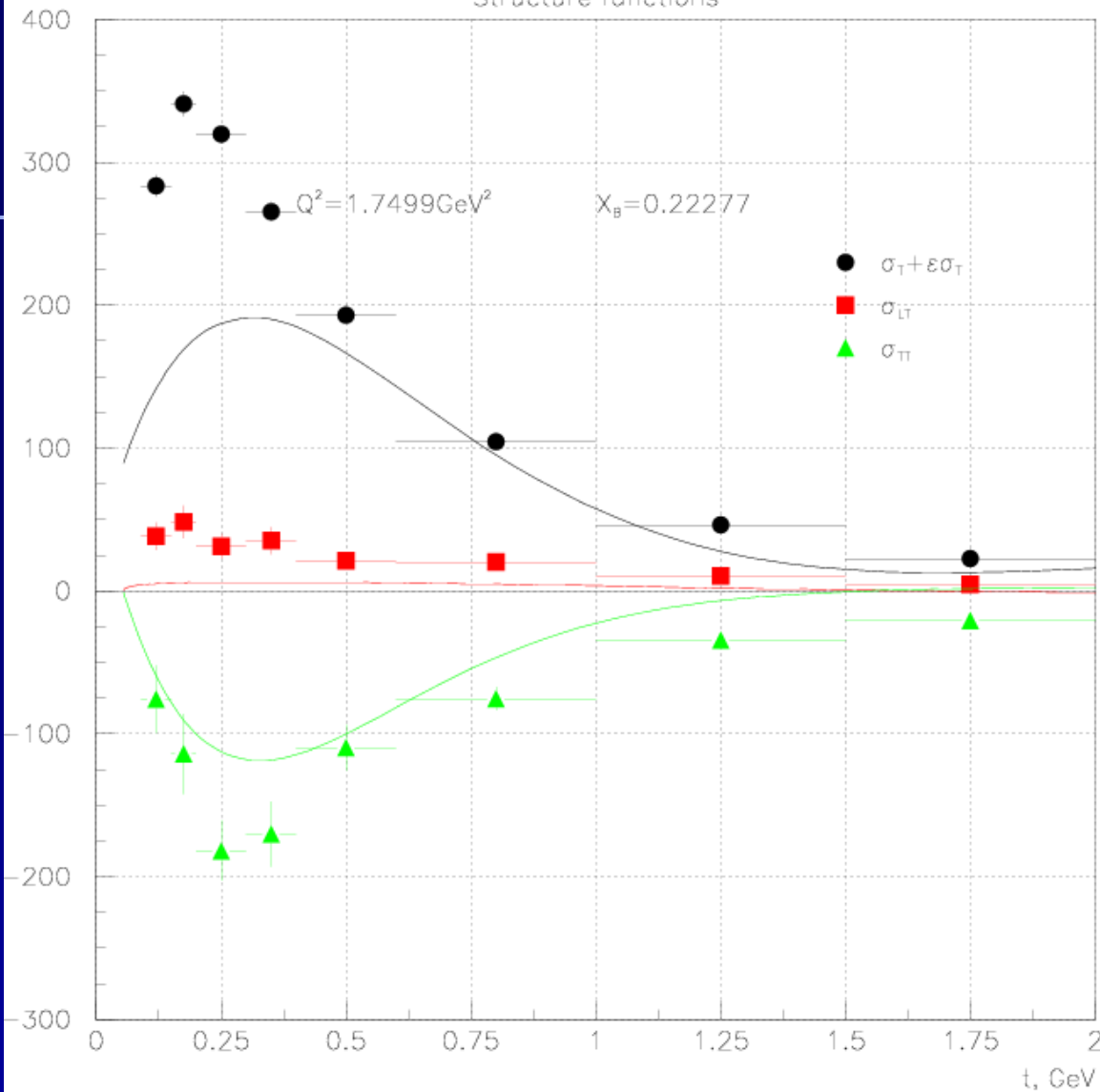
$Q^2 = 1.38 \text{ GeV}^2$
 $X_B = 0.17$

Structure functions

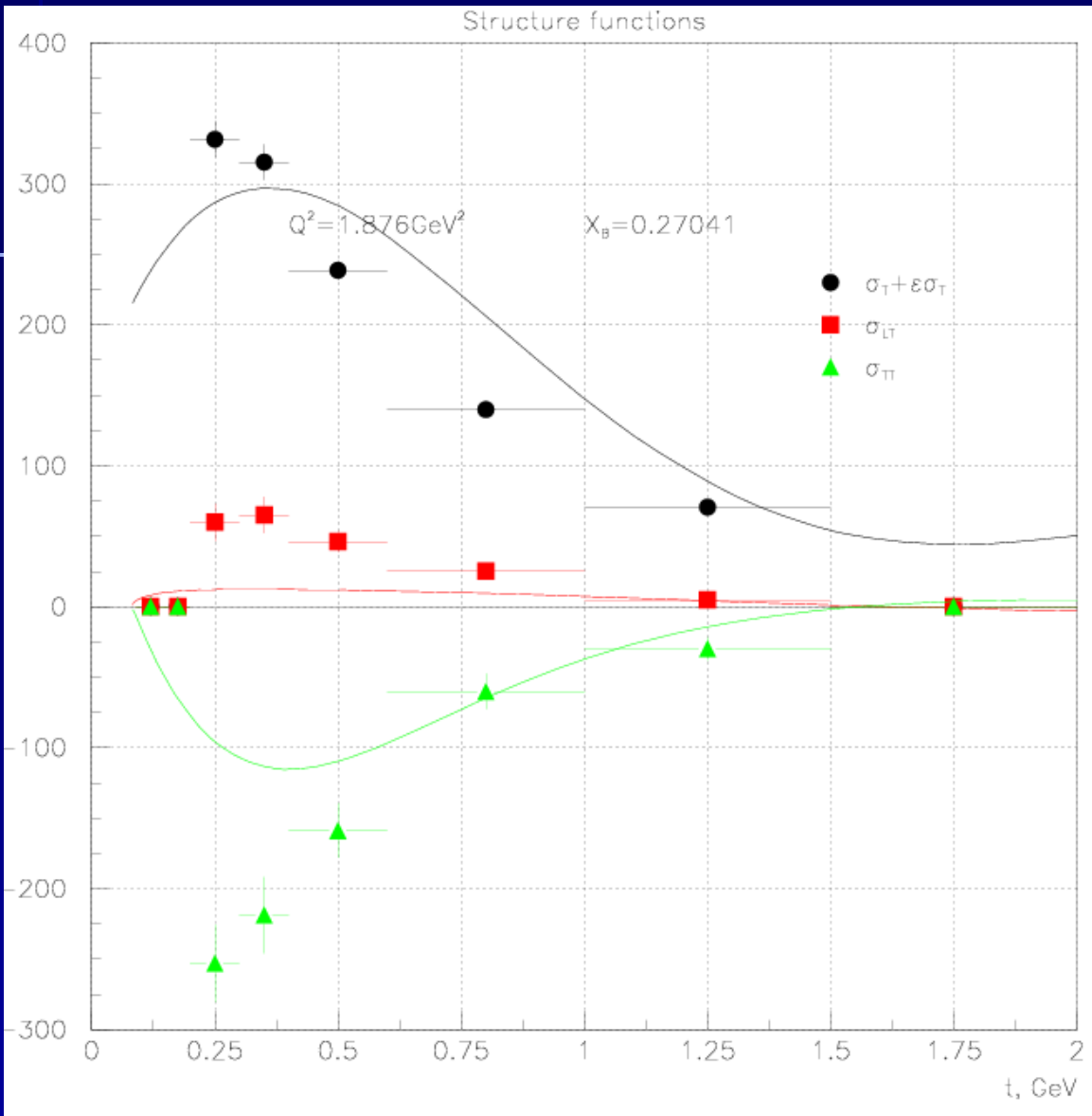


$Q^2 = 1.61 \text{ GeV}^2$
 $X_B = 0.19$

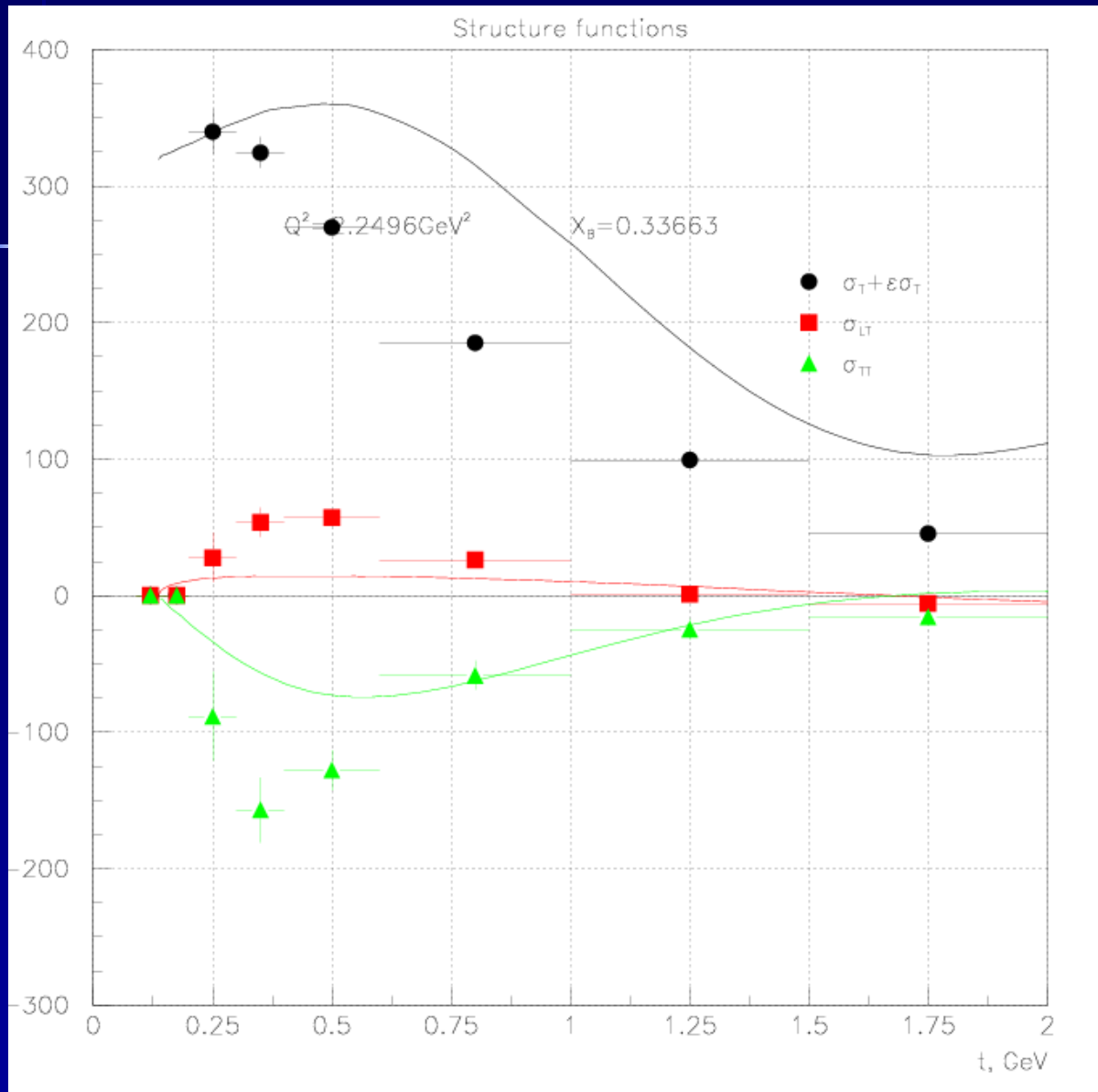
Structure functions



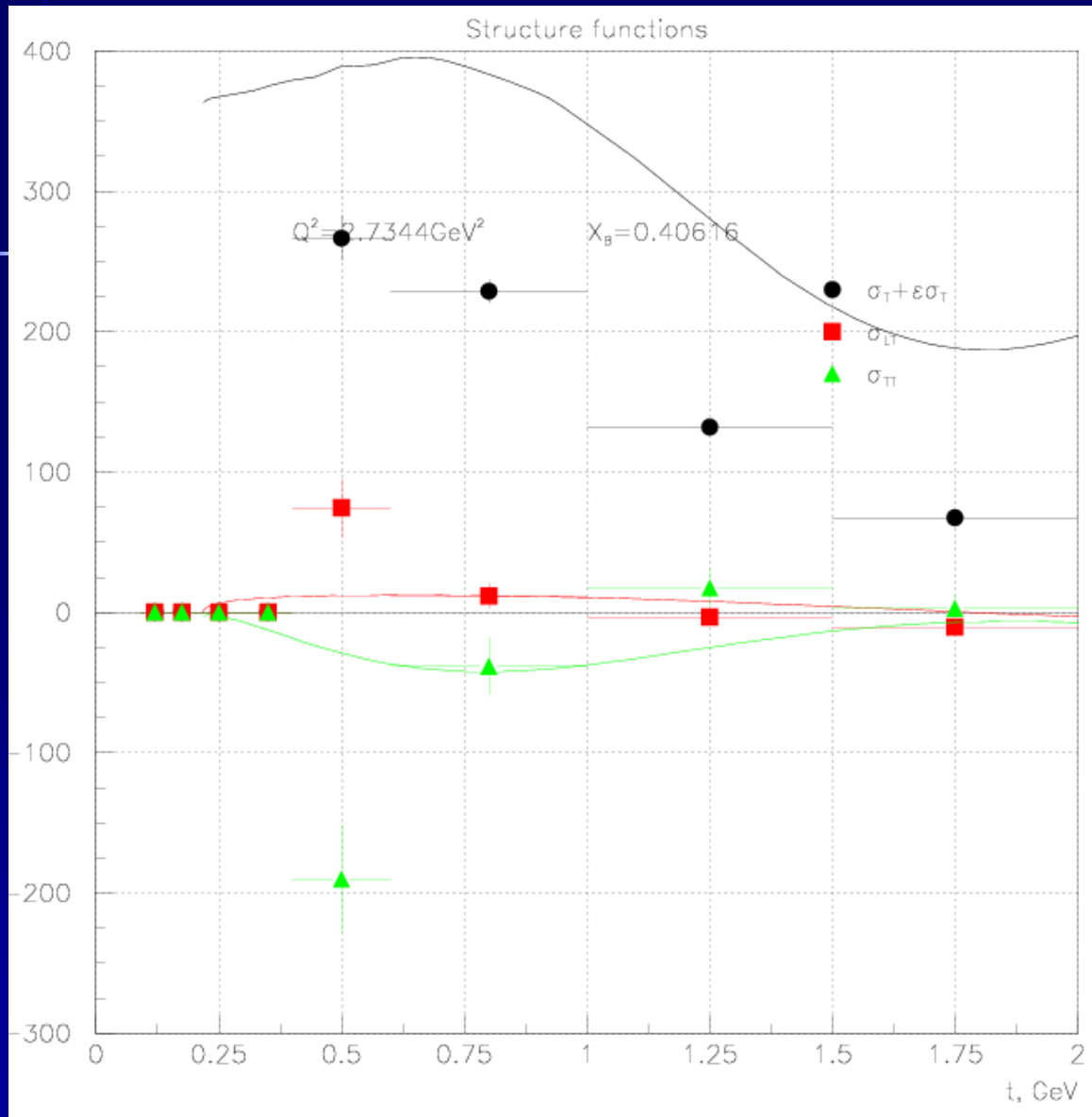
$Q^2 = 1.74 \text{ GeV}^2$
 $X_B = 0.22$



$Q^2 = 1.88 \text{ GeV}^2$
 $X_B = 0.27$

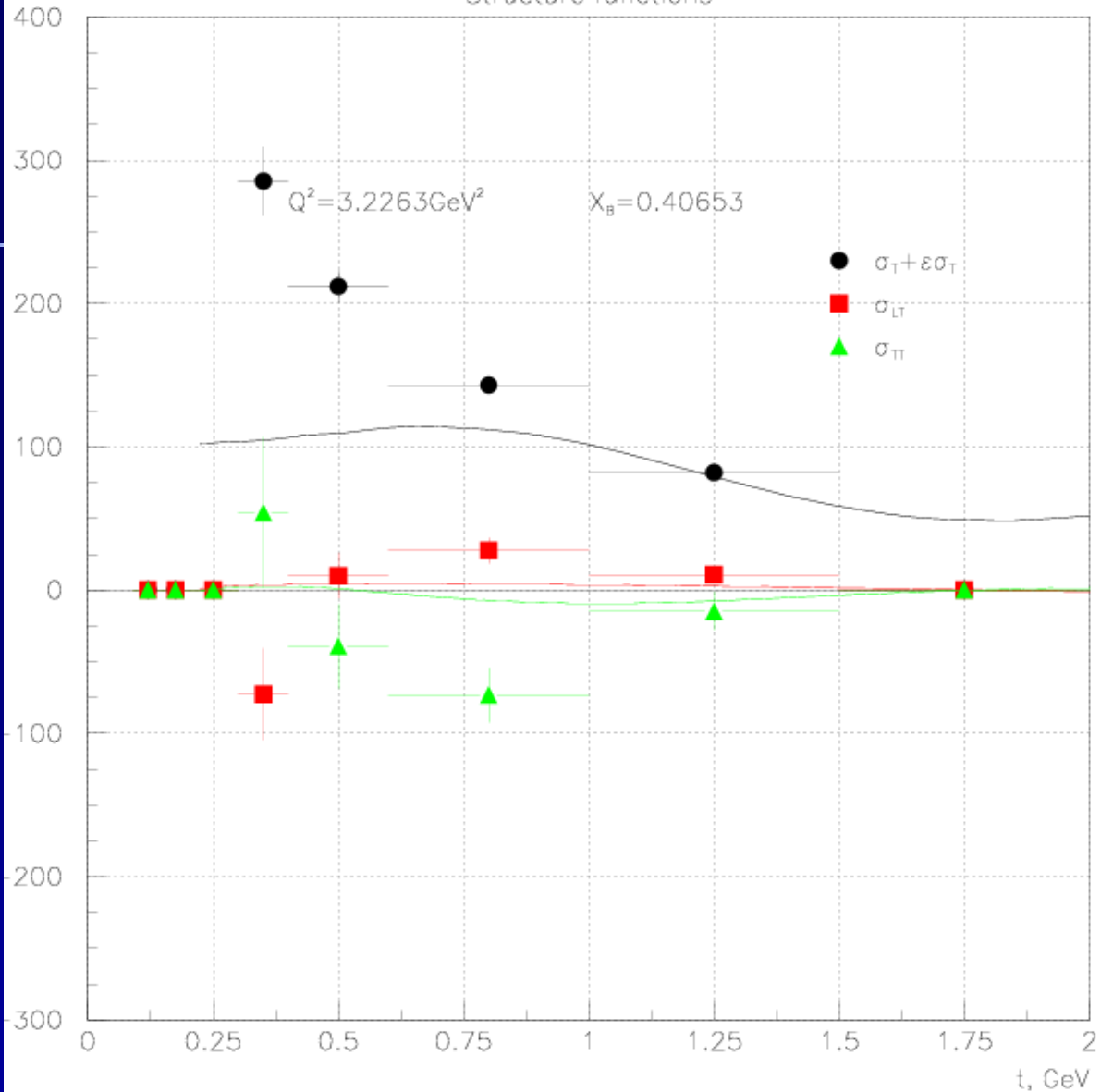


$Q^2 = 2.25 \text{ GeV}^2$
 $X_B = 0.34$



$Q^2 = 2.73 \text{ GeV}^2$
 $X_B = 0.41$

Structure functions

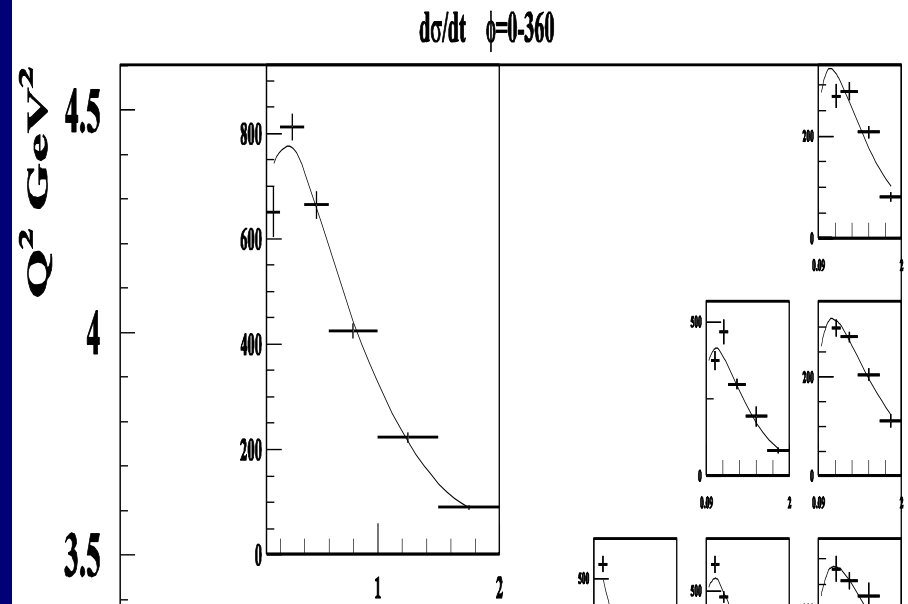


$Q^2 = 3.22 \text{ GeV}^2$
 $X_B = 0.41$

$$\gamma^* p \rightarrow p \pi^0$$

t - distribution

$$\frac{d\sigma}{dt} \propto e^{B(x_B, Q^2)t}$$



$$\gamma^* p \rightarrow p \pi^0$$

t-Slope Parameter as a Function of x_B and Q^2

$$\frac{d\sigma}{dt} \propto e^{B(x_B, Q^2)t}$$

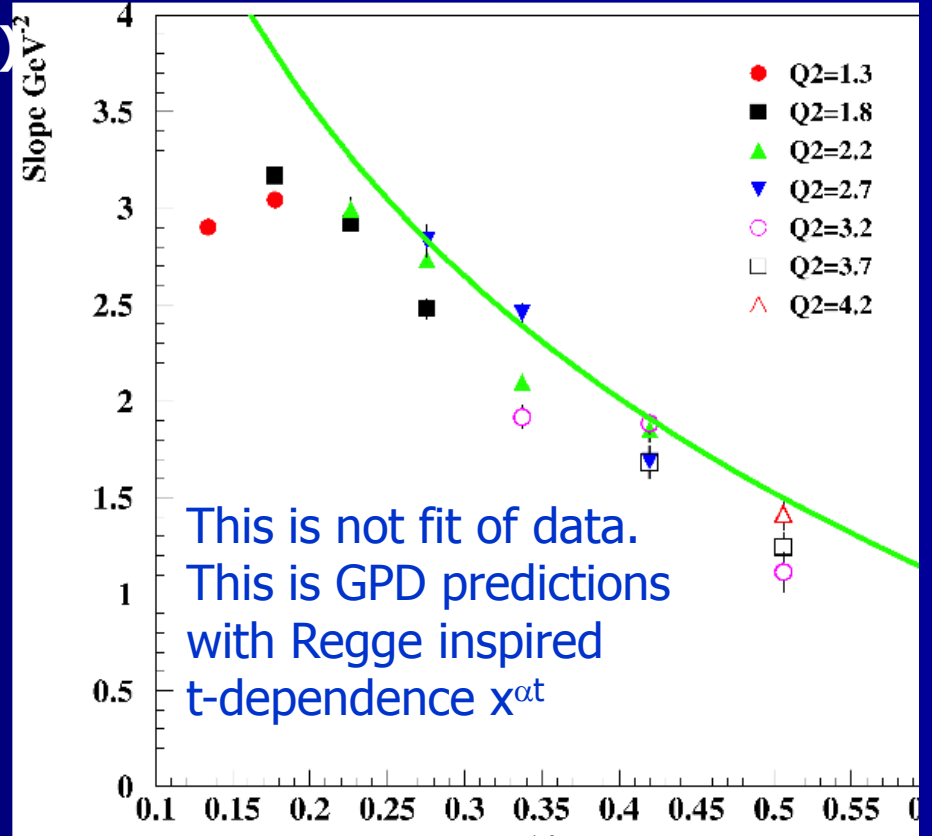
$B(x_B, Q^2)$

$$f^q(x, t) \propto x^{\alpha_q(t)} \propto x^{\alpha't}$$

$$\frac{d\sigma}{dt} \propto [x^{\alpha't}]^2 = e^{2\alpha' \ln(1/x)t}$$

$$B(x) = 2\alpha' \ln(1/x)$$

$$\alpha' = 1.1$$



- $B(x_B, Q^2)$ is almost independent of Q^2
- $B(x_B)$ is decreasing with increasing x_B

x_B

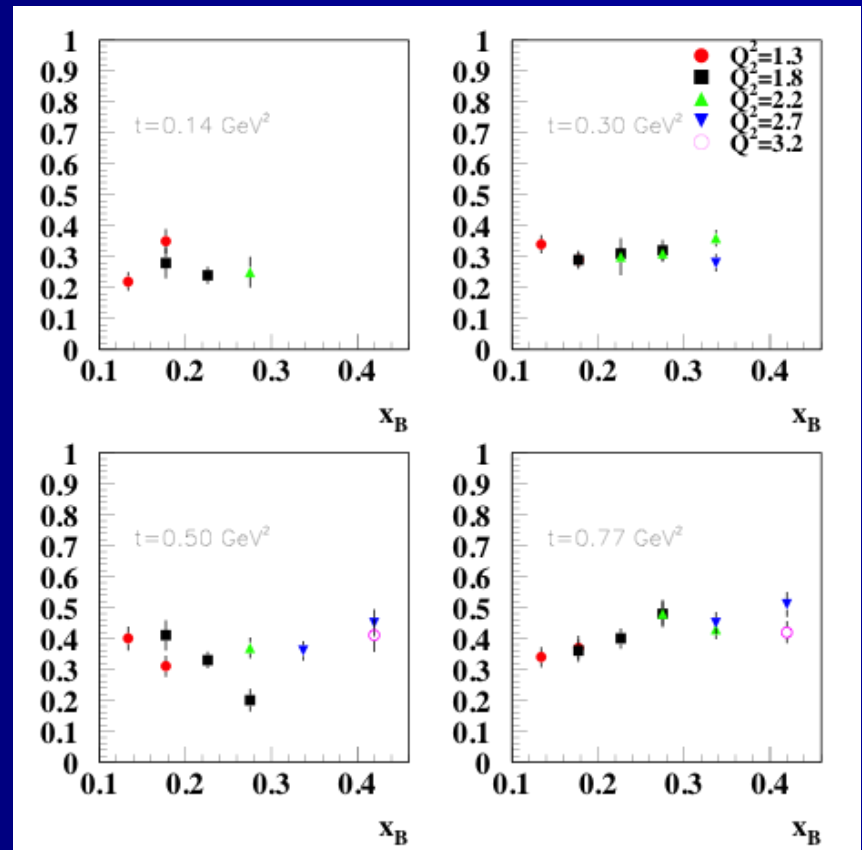
η/π^0 Ratio

$$\frac{\sigma(ep \rightarrow ep\eta)}{\sigma(ep \rightarrow ep\pi^0)}$$

Preliminary data on the ratio η/π^0 as a function of x_B for different bins in t .

The dependence on the x_B and Q^2 is very weak.

Probably we have small positive slope. The ratio in the photoproduction is near 0.2-0.3 (very close to what we have at our smallest Q^2).



π^0 and η Beam Spin Asymmetry

$$\frac{d\sigma}{dtd\phi}(Q^2, x, t, \phi) = \frac{1}{2\pi} \left(\frac{d\sigma_T}{dt} + \varepsilon \frac{d\sigma_L}{dt} + \varepsilon \frac{d\sigma_{TT}}{dt} \cos 2\phi + \sqrt{2\varepsilon(\varepsilon+1)} \frac{d\sigma_{LT}}{dt} \cos \phi \right. \\ \left. + h \sqrt{2\varepsilon(\varepsilon-1)} \sin \phi \frac{d\sigma_{LT}}{dt} \right)$$

h is the beam helicity

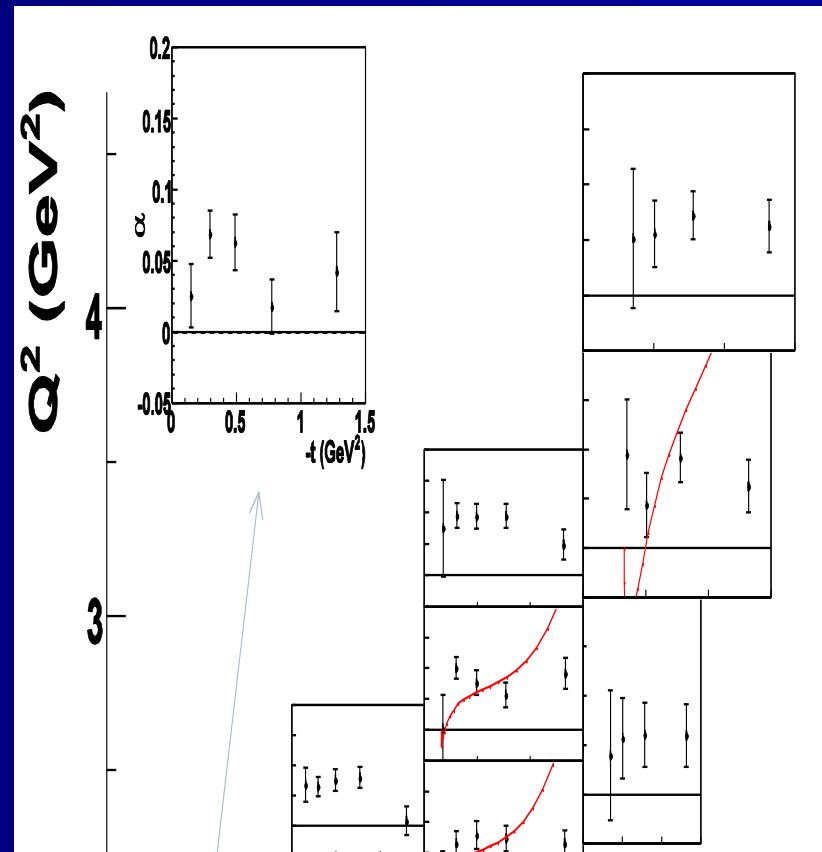
$$A = \frac{d^4 \vec{\sigma} - d^4 \bar{\sigma}}{d^4 \vec{\sigma} + d^4 \bar{\sigma}} \approx \alpha \sin \varphi$$

Any observation of a non-zero BSA would be indicative of an L'T interference. If σ_L dominates, σ_{LT} , σ_{TT} , and $\sigma_{L'T}$ go to zero

$$\gamma^* p \rightarrow p \pi^0$$

Beam Spin Asymmetry

- The red curves correspond to the Regge model (JML)
- BSA are systematically of the order of 0.03-0.09 over wide kinematical range in x_B and Q^2

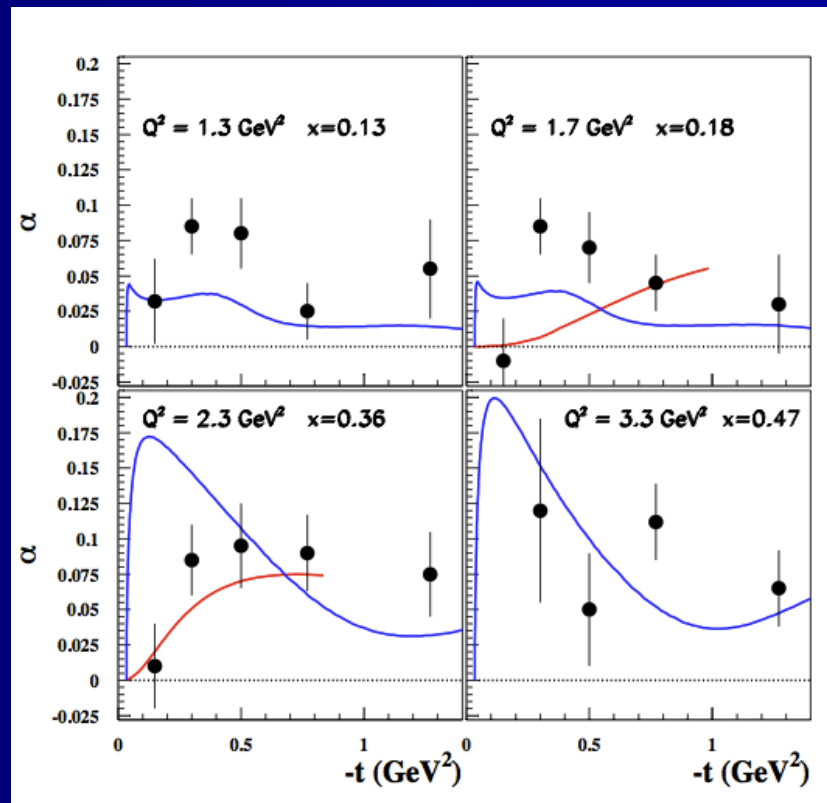


$$\gamma^* p \rightarrow p \pi^0$$

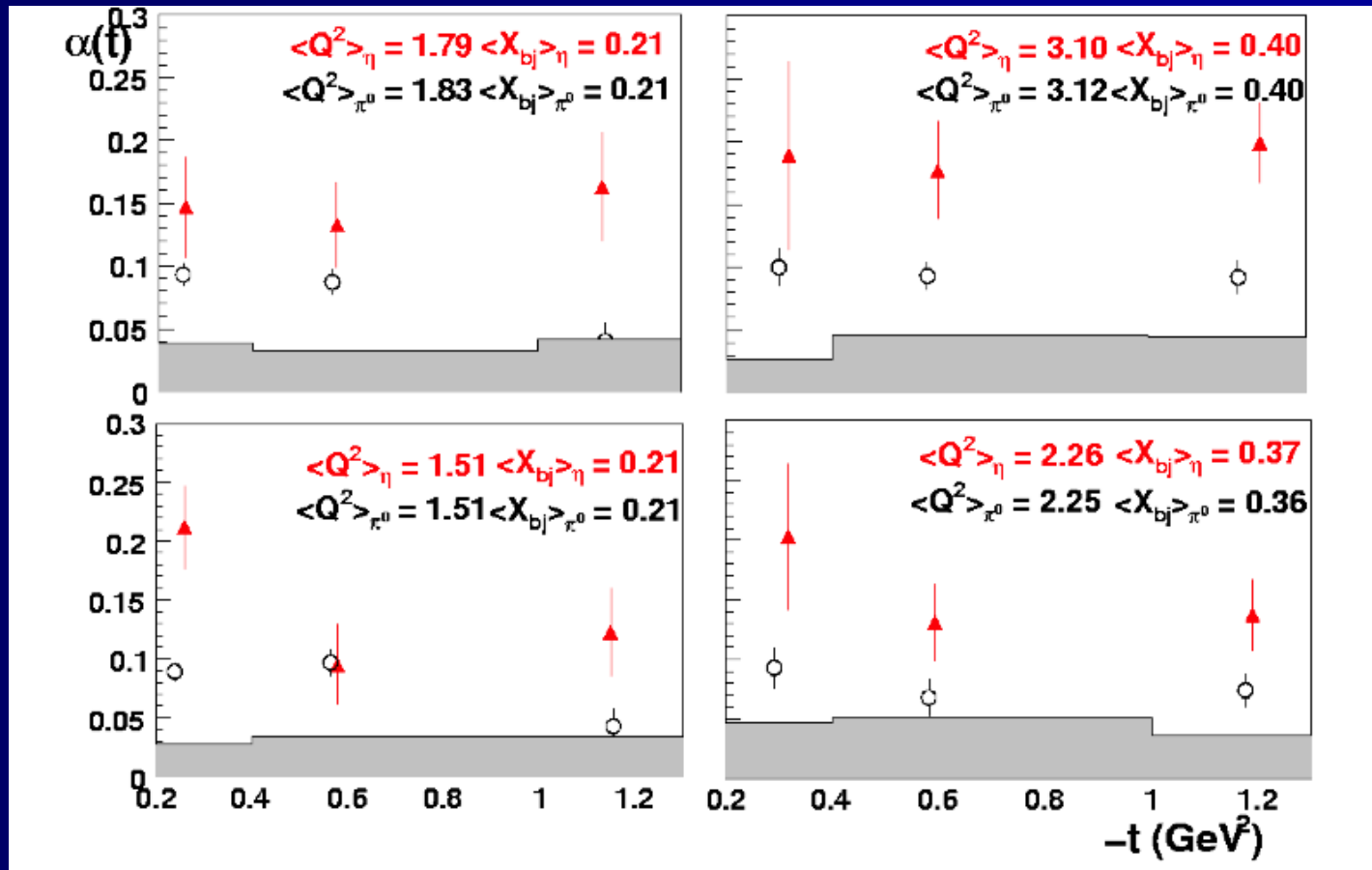
Beam Spin Asymmetry

Ahmad, Goldstein, Luiti, 2009

- Data CLAS
- Blue – Regge model
- Red – GPD predictions
- tensor charges
 $\delta u = 0.48,$
 $\delta d = -0.62$
- transverse anomalous magnetic moments
 $\kappa_T^u = 0.6,$
 $\kappa_T^d = 0.3.$



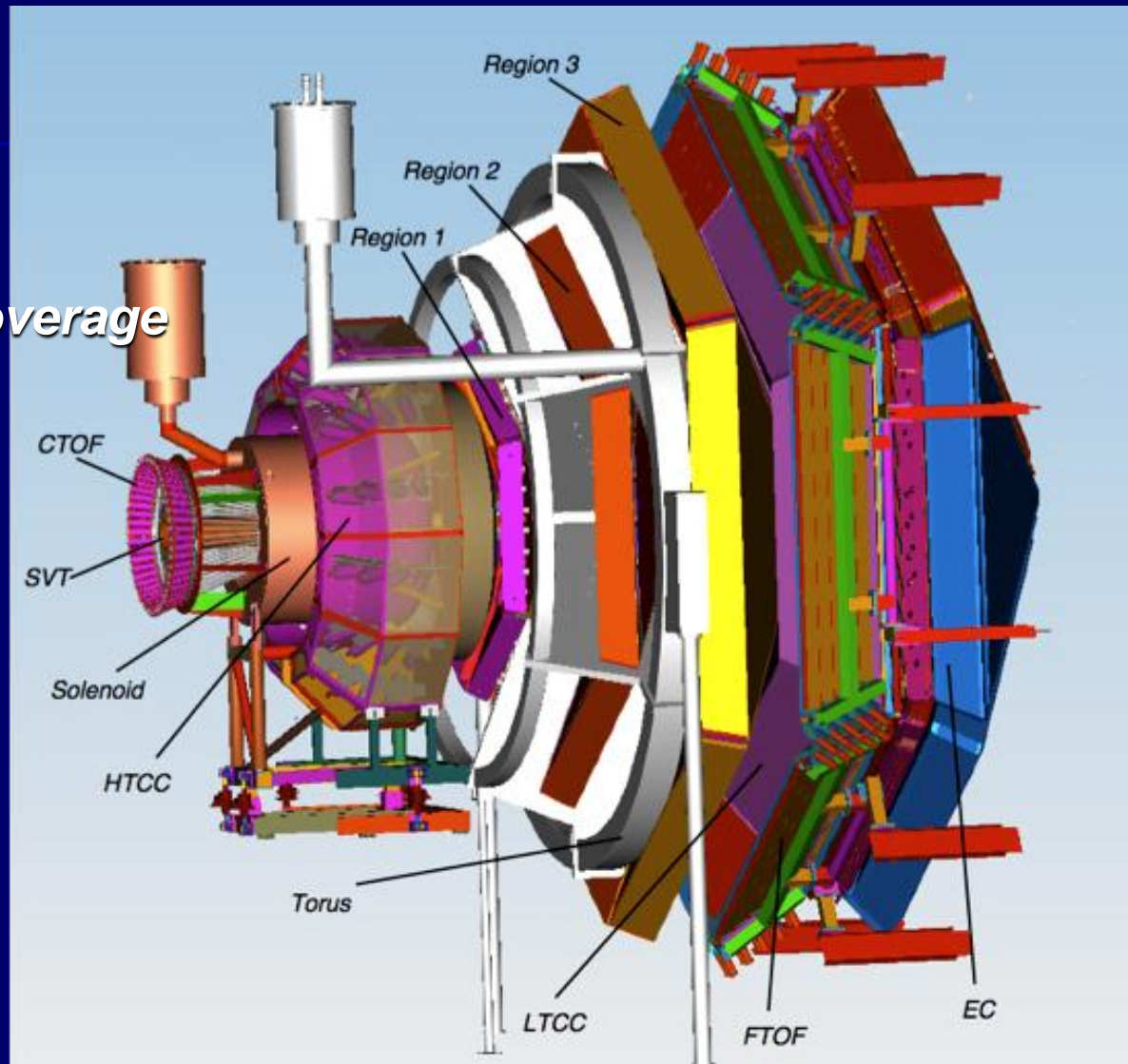
η Beam Spin Asymmetry



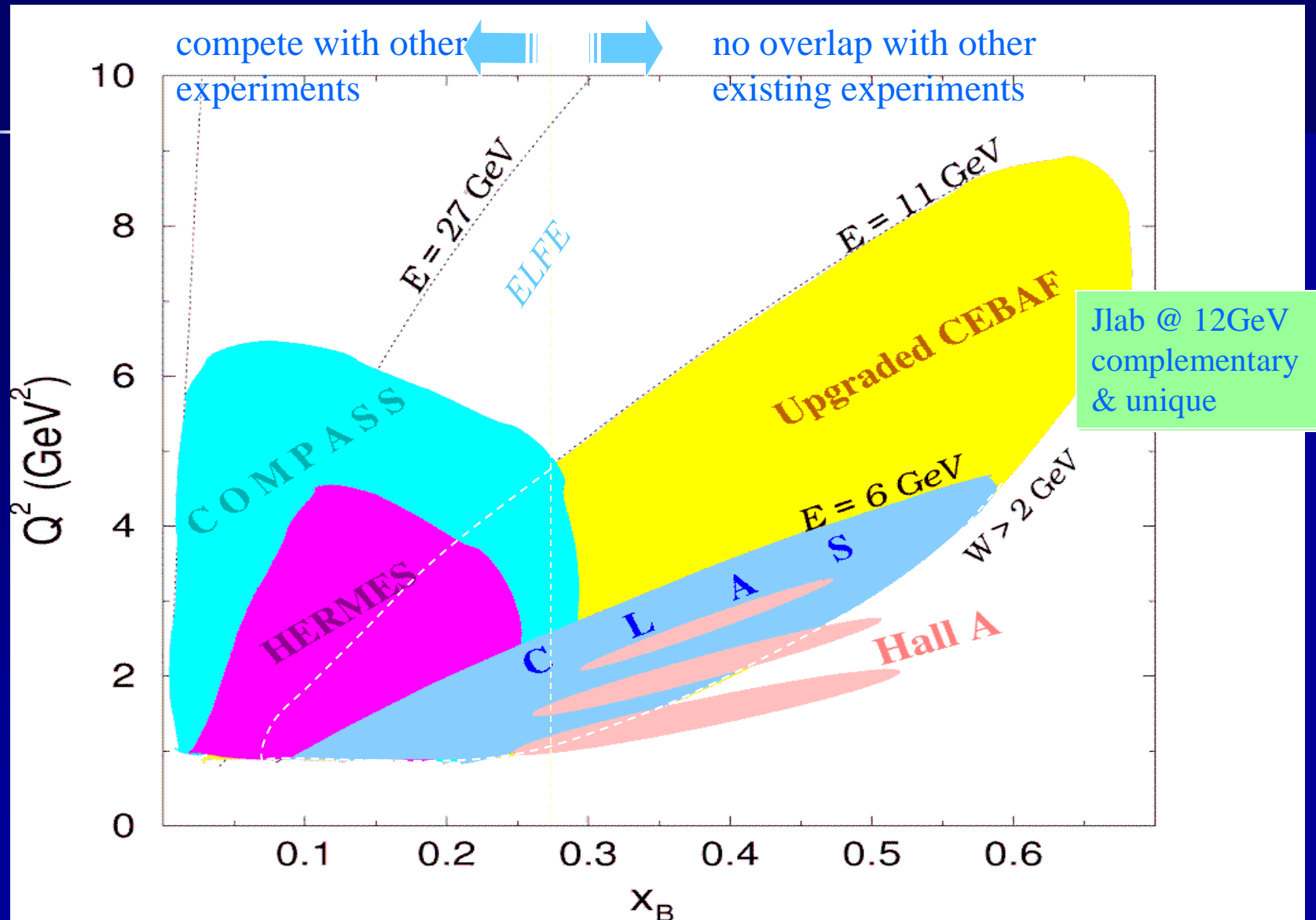
JLab 12 GeV Upgrade

CLAS12

- High luminosity
- Large acceptance
- Wide kinematic coverage
- High precision

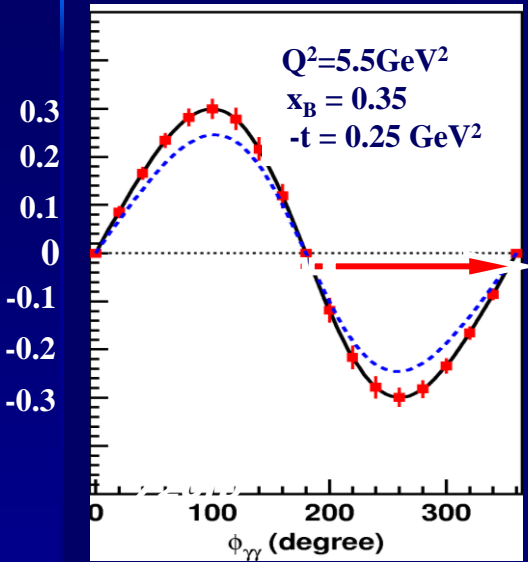


Kinematics coverage for deeply exclusive experiments

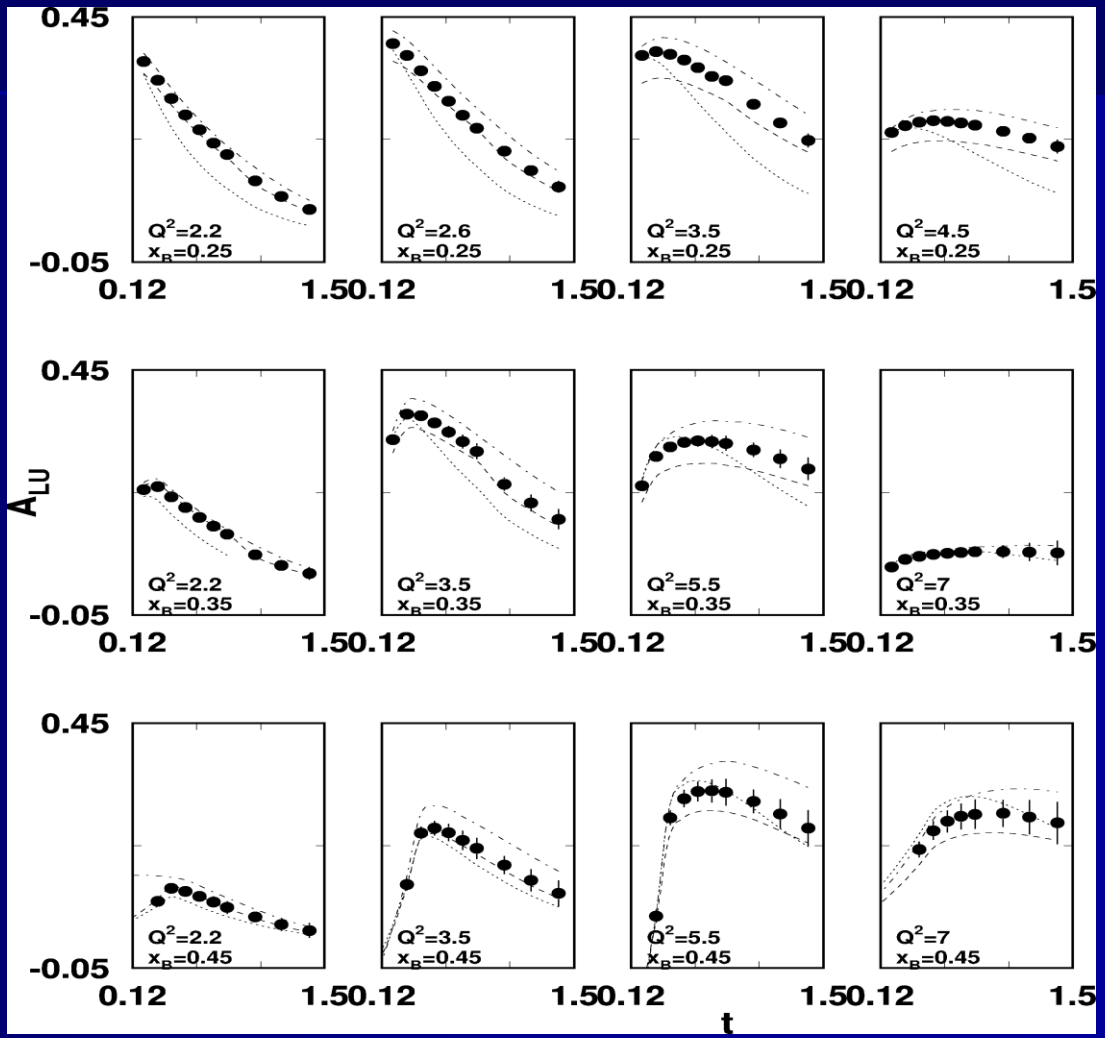


DVCS beam asymmetry at 12 GeV

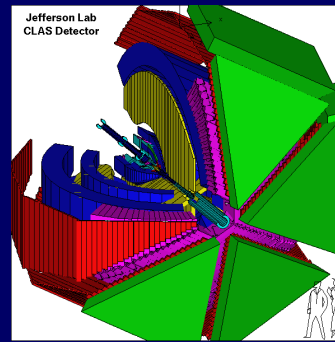
$$ep \rightarrow epy$$



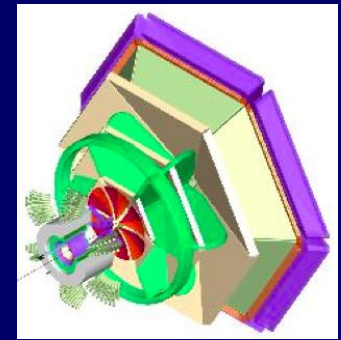
Kinematics coverage,
 $Q^2 < 8 \text{ GeV}^2$,
 $x_B < 0.65$,
 $t < 2.0 \text{ GeV}^2$



Summary

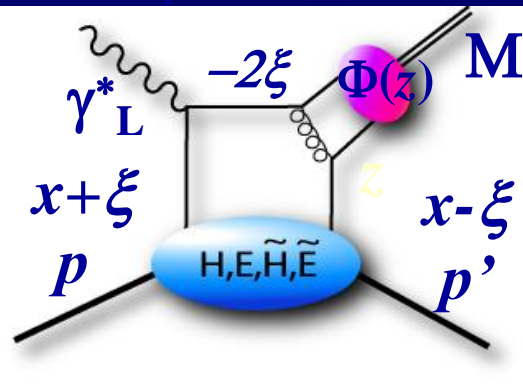


2015

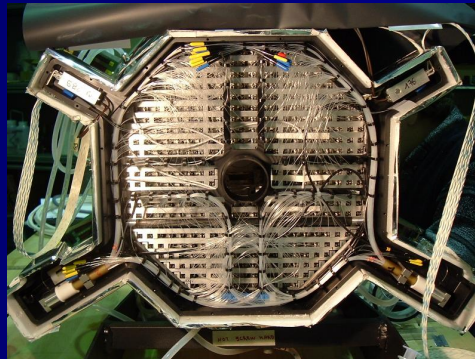


- Deeply Virtual Meson Production has the potential to probe the nucleon structure at the parton level, as described by Generalized Parton distributions (GPDs).
- The most extensive set of π^0 , η , ρ^+ , ρ^0 , ω , and ϕ electroproduction to date has been obtained with the CLAS spectrometer.
- Structure functions, the π^0/η ratio of the cross sections and beam-spin asymmetries were extracted in the valence quark region.
- Sizable interference terms σ_{TT} and σ_{LT} and non-zero asymmetries imply that both transverse and longitudinal amplitudes participate in the process.
- The detailed comparison with the Regge model predictions was done. The model describes the data reasonably well.
- We are working with theorists who are doing the calculation of the DVMP cross sections within the handbag GPD based models. The comparison results are coming.
- CLAS12 will continue the GPD study with broader kinematics at 12 GeV machine.

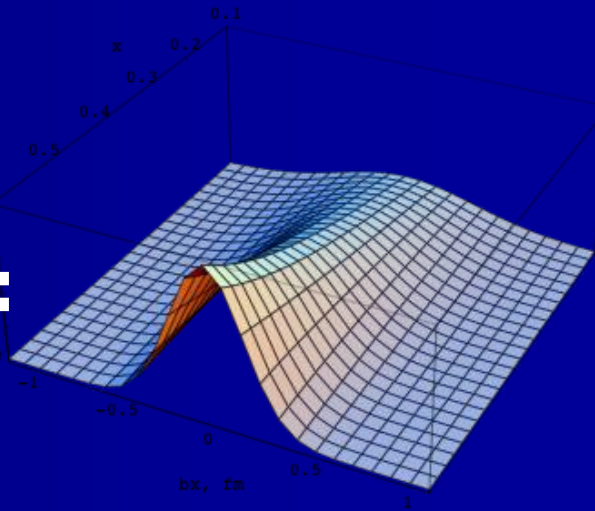
The End



+

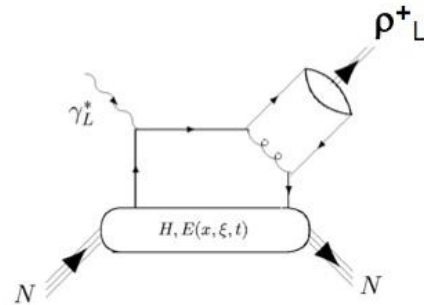


=



Vector mesons

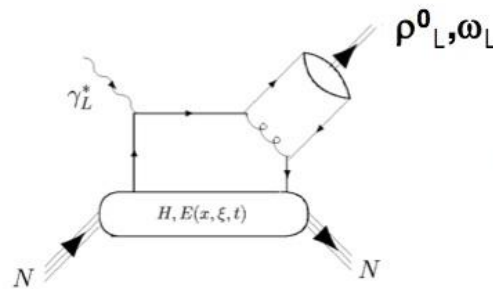
$$\gamma^* p \rightarrow n \rho^+$$



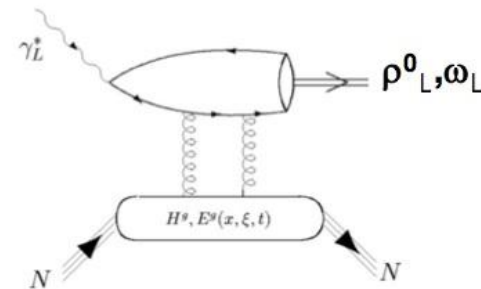
ρ^0	$e_u H^u - e_d H^d$ $e_u E^u - e_d E^d$
ω	$e_u H^u + e_d H^d$ $e_u E^u + e_d E^d$
ρ^+	$H^u - H^d$ $E^u - E^d$

$$\gamma^* p \rightarrow p \rho^0$$

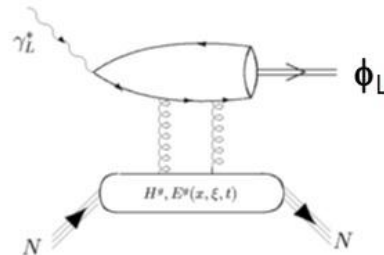
$$\gamma^* p \rightarrow p \omega$$



+

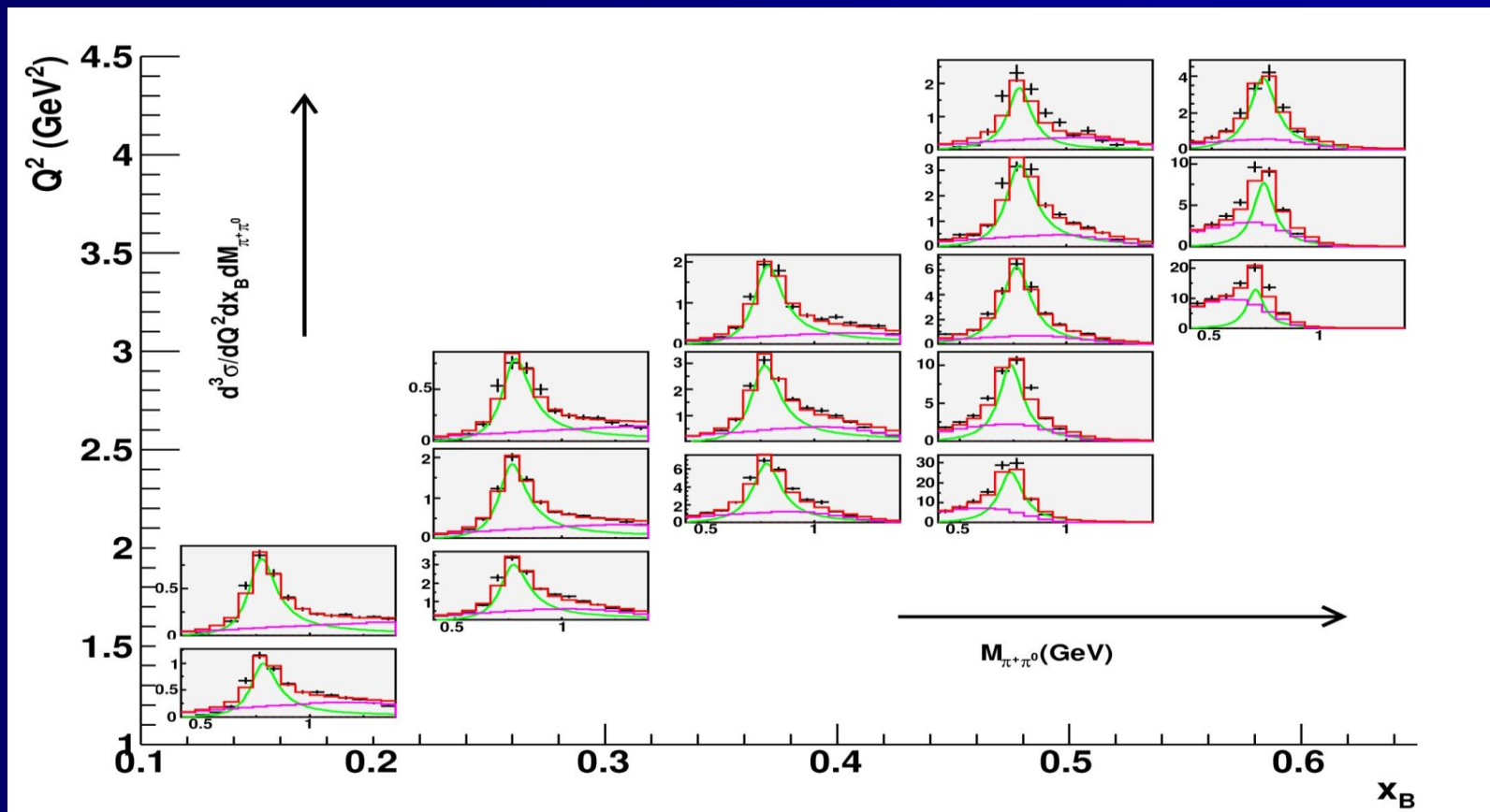


$$\gamma^* p \rightarrow p \phi$$



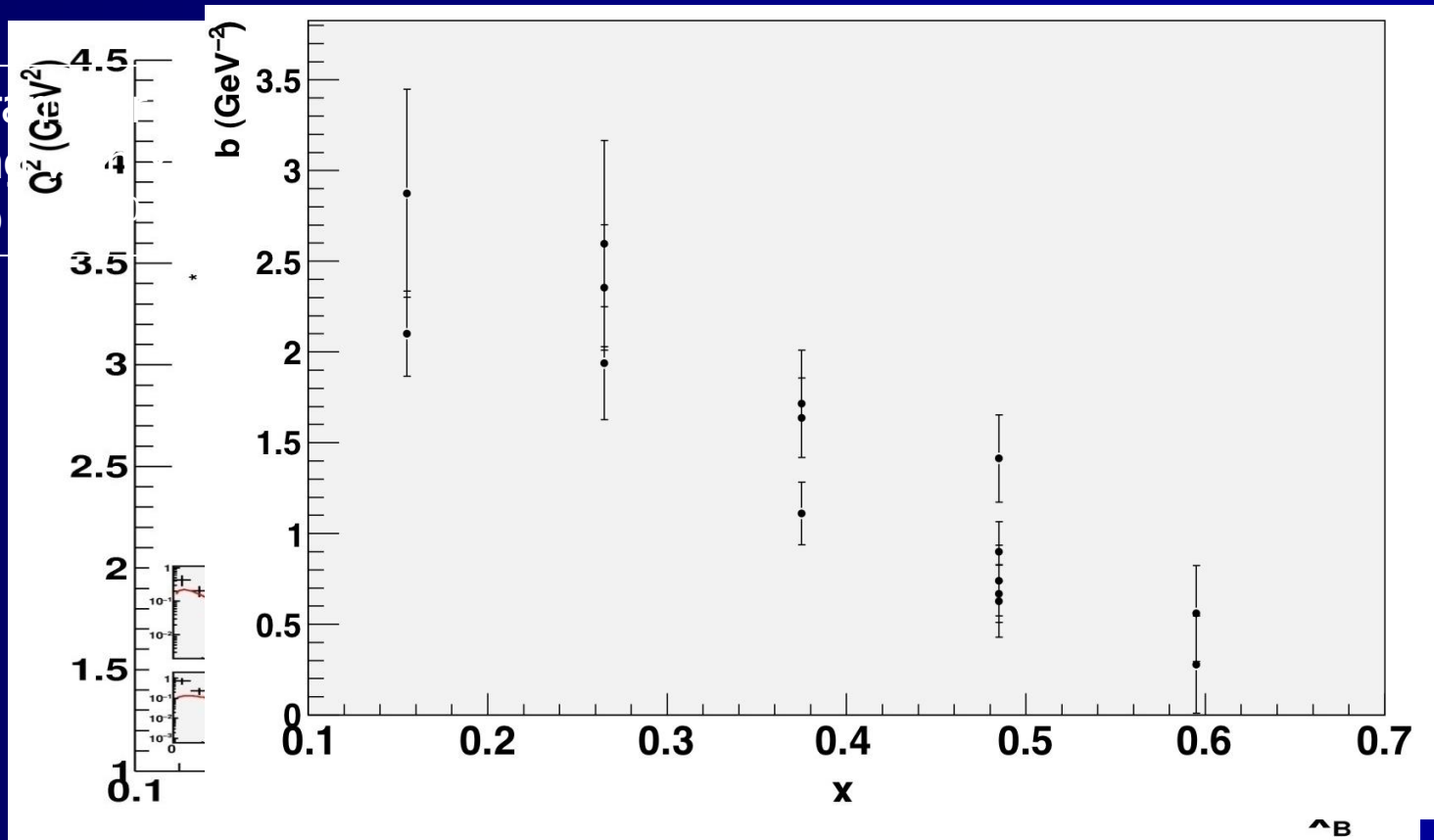
$$ep \rightarrow en\rho^+, \quad \rho^+ \rightarrow \pi^+\pi^0, \quad \pi^0 \rightarrow \gamma\gamma$$

World's first-ever measurement



$$\frac{d\sigma}{dt}(\gamma^* p \rightarrow en\rho^+) \propto \sqrt{-t} e^{bt}$$

Slope parameter
decreasing
Similar to

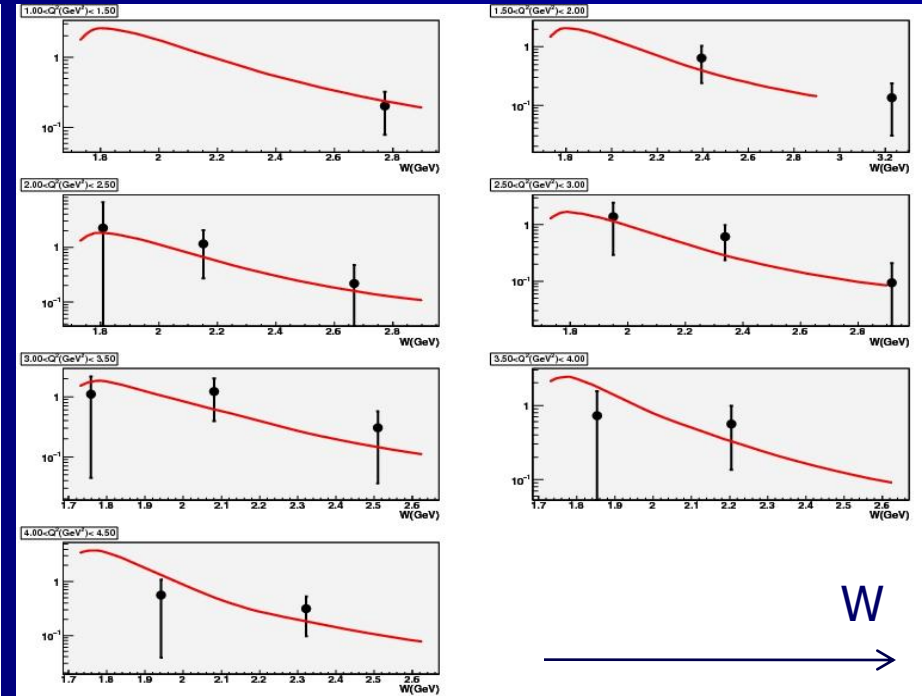
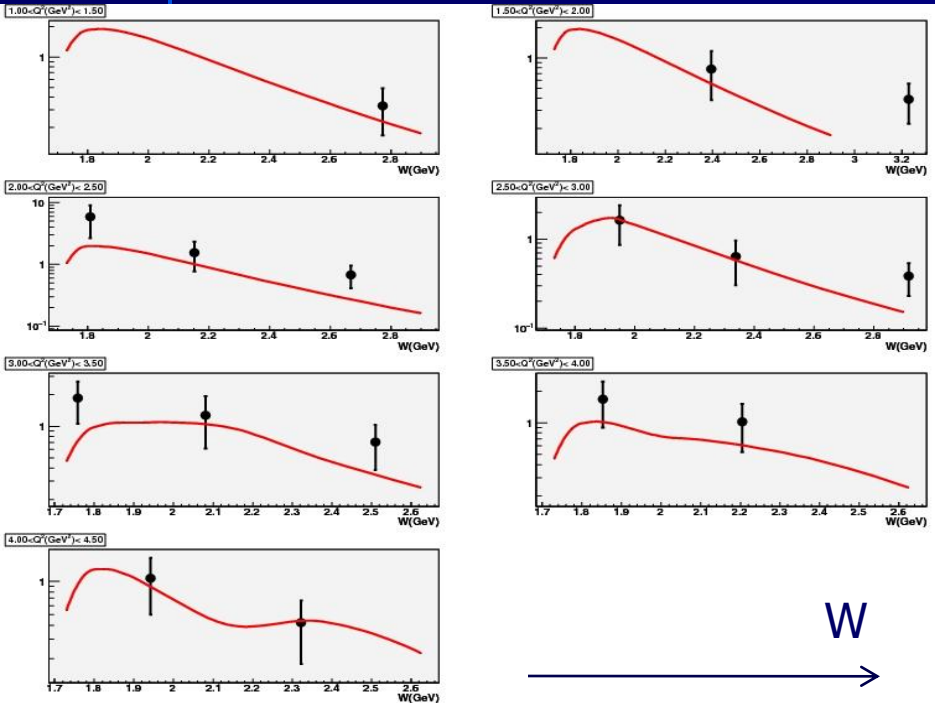


σ_L σ_T separation

SCHC S-channel helicity conservation

σ_L

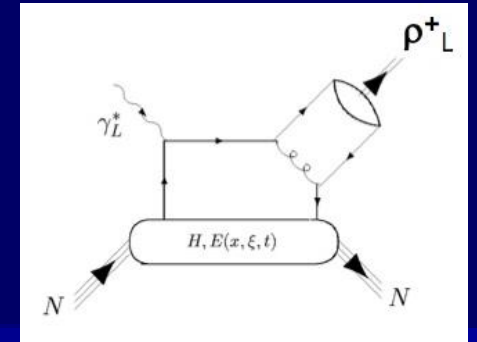
σ_T



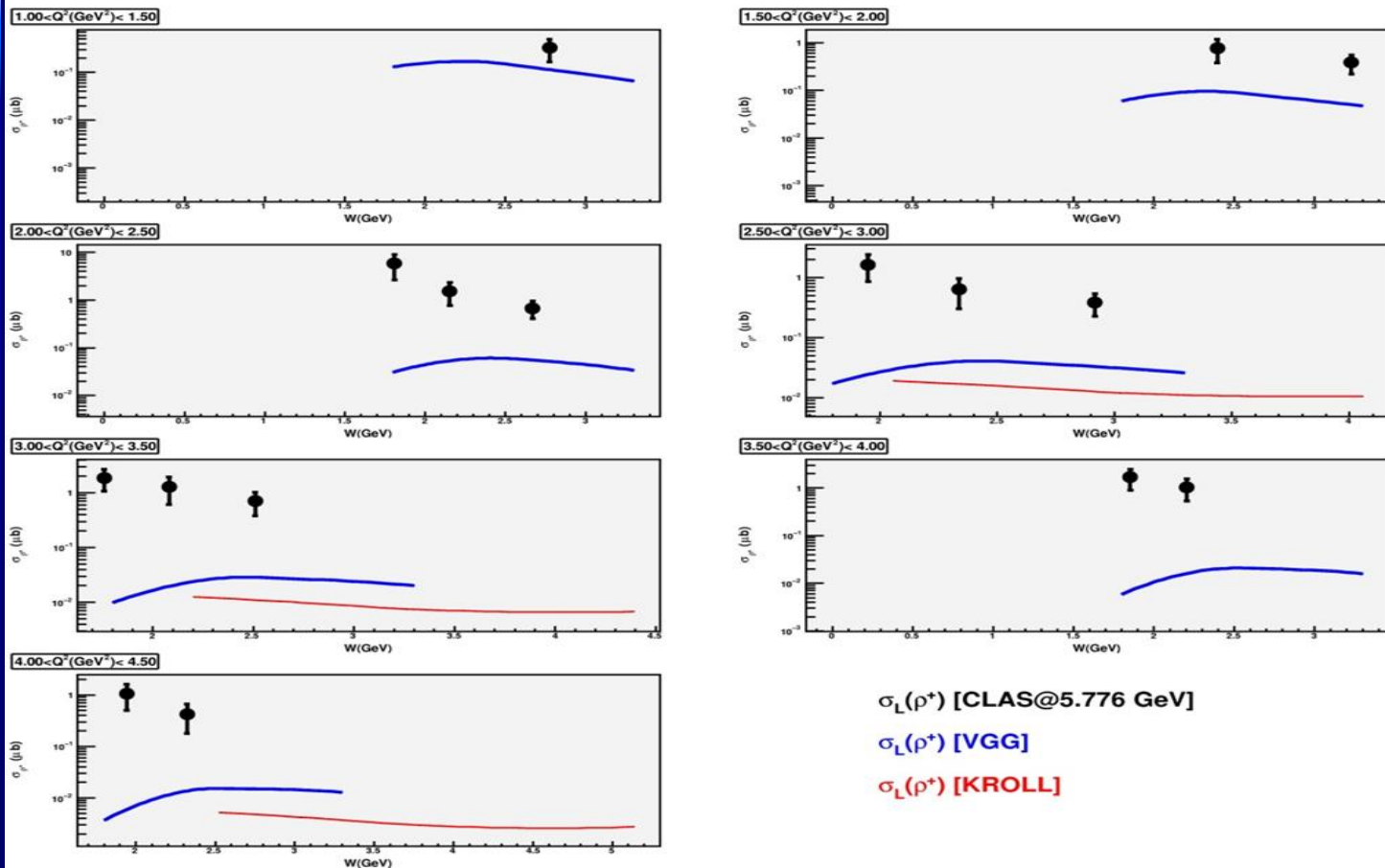
Red lines (Regge model) :Laget, Phys. Rev. D 65, 074022 (2002)

$$\gamma_L^* p \rightarrow p \rho^+$$

CLAS data

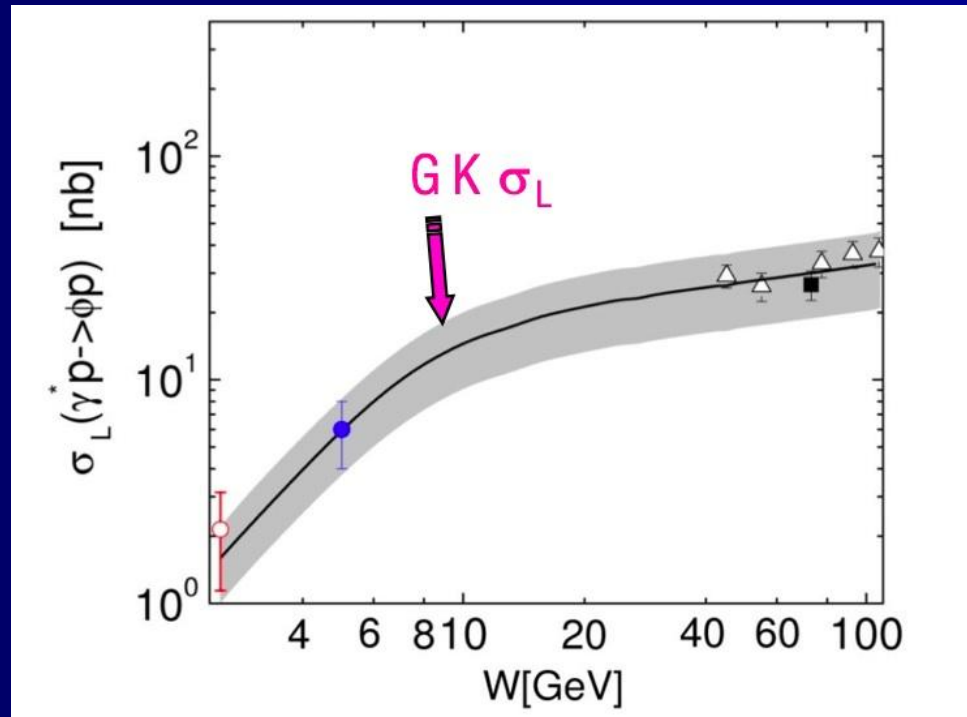
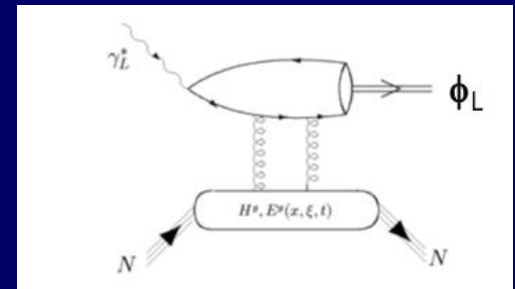


σ_L



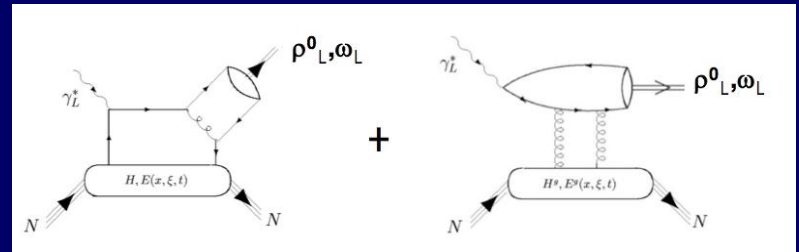
GPD fails to describe data by more than order of magnitude

$$\gamma_L^* p \rightarrow p \phi$$



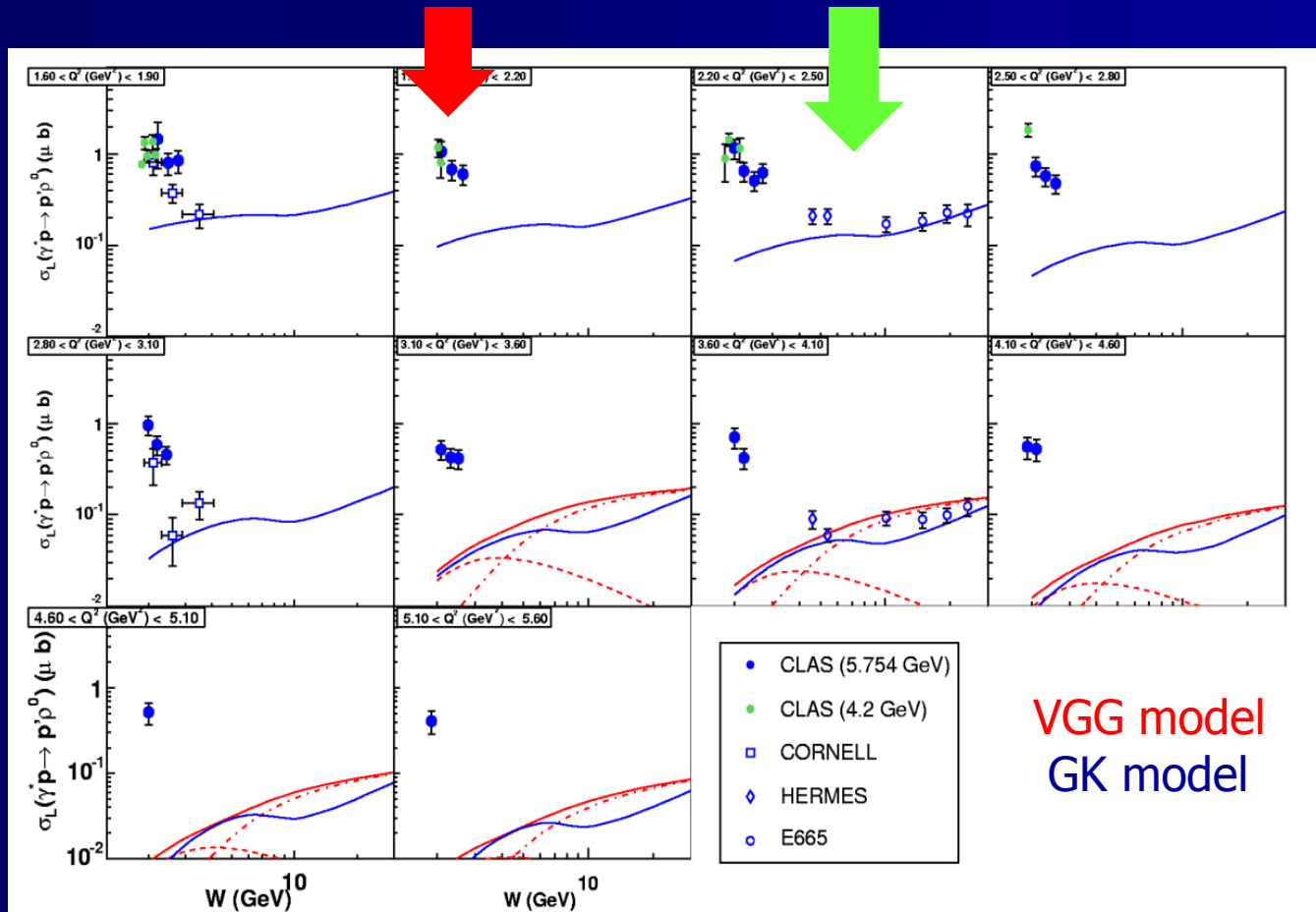
- Gluons GPD are dominant for ϕ mesons
- GPD approach describes well data for $W > 5$ GeV
- for ρ^0 and ω channels: handbag for sea quarks and/or gluons is dominant.

$$\gamma_L^* p \rightarrow p \rho^0$$

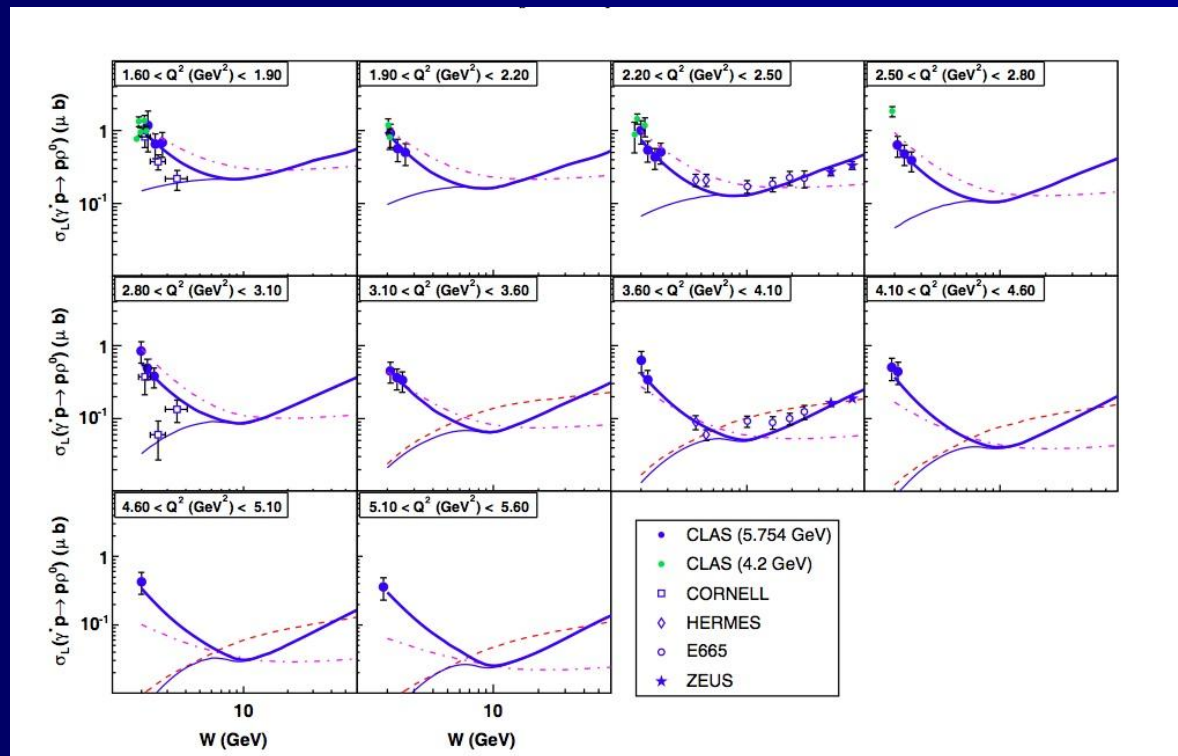


Fails to describe data $W < 5$ GeV

Describes well for $W > 5$ GeV



VGG "meson-like contribution"



- Popular GK and VGG models can not provide the right W -dependence of the cross-section
- This does not mean that we can't access GPD in vector meson electroproduction
- For example, adding the so called generalized D-term together with standard VGG model successfully describes data

Summary

- CLAS DVCS results were used for the GPD extraction. This is the first step in 3-D imaging of the nucleon
- More data coming with H₂ and polarized targets.
- The most extensive data set of π^0 , η , ρ^+ , ρ^0 , ω , and ϕ electroproduction to date has been obtained with the CLAS spectrometer
- Cross sections and beam-spin asymmetries were extracted in the valence quark region
- The detailed comparison with the Regge model predictions was done. The model describes the data reasonably well
- The popular GPD models fail to describe the experimentally measured meson cross sections. The present data provide important input to improve our understanding of these fundamental QCD issues
- CLAS12 will continue the GPD study with broader kinematics at 12 GeV machine

